AD_____

Award Number: W81XWH-04-1-0436

TITLE: Characterizing a Rat Brca2 Knockout Model

PRINCIPAL INVESTIGATOR: Michael N. Gould, Ph.D.

CONTRACTING ORGANIZATION: University of Wisconsin
Madison, Wisconsin 53706-1490

REPORT DATE: May 2007

TYPE OF REPORT: Final

PREPARED FOR: U.S. Army Medical Research and Materiel Command
Fort Detrick, Maryland 21702-5012

REPORT DOCUMENTATION PAGE

Form Approved
OMB No. 0704-0188

1. REPORT DATE *(DD-MM-YYYY)*	**2. REPORT TYPE**	**3. DATES COVERED** *(From - To)*
01-05-2007	Final	14 Apr 2004 – 13 Apr 2007

4. TITLE AND SUBTITLE

Characterizing a Rat Brca2 Knockout Model

5a. CONTRACT NUMBER

5b. GRANT NUMBER
W81XWH-04-1-0436

5c. PROGRAM ELEMENT NUMBER

6. AUTHOR(S)

Michael N. Gould, Ph.D.

E-Mail: gould@oncology.wisc.edu

5d. PROJECT NUMBER

5e. TASK NUMBER

5f. WORK UNIT NUMBER

7. PERFORMING ORGANIZATION NAME(S) AND ADDRESS(ES)

University of Wisconsin
Madison, Wisconsin 53706-1490

8. PERFORMING ORGANIZATION REPORT NUMBER

9. SPONSORING / MONITORING AGENCY NAME(S) AND ADDRESS(ES)
U.S. Army Medical Research and Materiel Command
Fort Detrick, Maryland 21702-5012

10. SPONSOR/MONITOR'S ACRONYM(S)

11. SPONSOR/MONITOR'S REPORT NUMBER(S)

12. DISTRIBUTION / AVAILABILITY STATEMENT
Approved for Public Release; Distribution Unlimited

13. SUPPLEMENTARY NOTES

14. ABSTRACT

Brca2 mutation carriers, while rare in the population, have a high probability to develop breast cancer. In order to better understand the etiology of this disease, as well as to develop pre-vention and treatment strategies for it, we require good animal models. In this project we character-ized the first rat knockout produced, which was that of the Brca2 locus. We showed that Brca2-/- rats survive and develop multiple cancers, but not breast cancer. The lack of breast cancer was likely due to a Brca2-/- associated lack of ovarian follicular development. We developed two approaches to address this problem using inbred WF rats on which this knockout allele was placed. The first involved trans-planting wild-type ovaries to knockout rats. Brca2-/- rats having wild type ovaries did not develop mammary carcinomas, due to regression of the transplanted tissue over time. The alternative strategy was to transplant mammary glands from Brca2-/- rats into wild type rats. Brca2-/- mammary glands did not develop carcinomas when transplanted into wild type recipients. However their morphologic characteris-tics differed from wild type transplants, showing a higher degree of branching and lobularity. As an alternative to these transplant models, we induced mammary carcinomas in Brca2+/- and Brca2+/+ controls with 7,12,dimethylbenz(a)anthracene (DMBA) and nitrosomethylurea (NMU), but found no differences in tumor multiplicity between the two genotypes. Although we were unable to produce a mammary tumor model, the Brca2-/- knockout rat provides a valuable complement to existing mouse models to study the tissue-specific functions of the Brca2 protein.

15. SUBJECT TERMS
Brca2; breast; mammary; rat model; knockout

16. SECURITY CLASSIFICATION OF:			**17. LIMITATION OF ABSTRACT**	**18. NUMBER OF PAGES**	**19a. NAME OF RESPONSIBLE PERSON**
a. REPORT	**b. ABSTRACT**	**c. THIS PAGE**			USAMRMC
U	U	U	UU	51	**19b. TELEPHONE NUMBER** *(include area code)*

Table of Contents

INTRODUCTION

Carriers of mutations in the *BRCA2* gene have increased risk for developing cancers of the breast, ovary, colon and pancreas. In general, carriers are defined as individuals with protein truncating mutations within the *Brca2* allele. Many *Brca2* knockout lines have been produced and characterized in the mouse. Mutations that truncate the protein to remove exon 11 and downstream exons always result in lethality. The mouse knockout truncating *Brca2* the farthest 5' (after the third exon 11 BRC repeat) allows a very limited number of pups to survive to adulthood. In contrast, the rat *Brca2* knockout we produced was predicted to truncate the protein upstream of the corresponding mouse knockout, leaving only 2 modestly conserved BRC repeats. For this rat line, *Brca2* homozygous knockouts are 100% viable (1). The first six litters from the founder rat 3983 produced 35 heterozygous knockouts out of 64 N2 pups, demonstrating the Mendelian inheritance of this knockout gene in N2 pups. *Brca2* heterozygous N2 male and female rats were bred to produce *Brca2* homozygous knockout pups. The first set of N2F1 pups produced included 54 male and 58 female pups. The ratio of *Brca2* homozygous knockout rats to *Brca2* heterozygous and wild-type rats was approximately 1:2:1. Body weight data were collected for all N2F1 pups starting at weaning and show a clear phenotype of growth inhibition of male and female *Brca2* homozygous knockout rats. These rats are sterile and reduced in size but otherwise healthy up to ~6 months of age. Histopathological analysis of gonads from the *Brca2* homozygous male and female rats shows severe atrophy that is not observed in the *Brca2* heterozygous and wild-type rat gonads (2). The goals of this proposal were to characterize this first-ever rat knockout, which is for *Brca2*, as an *in vivo* model and on a cellular level. We also used this model to begin to address one of the most important unanswered questions regarding the *Brca* genes – what accounts for the organ specificity of carcinogenesis resulting from the full or partial inactivation of the Brca proteins?

BODY

The goals of this project were to be accomplished by the following specific aims:
Aim 1: Rat *Brca2* knockouts will be characterized as an *in vivo* model. (a) It is critical to determine if the *Brca2* knockout rats will develop mammary carcinomas. Female rats with the *Brca2* knockout allele on the SD and WF background strains will be followed with and without hormonal (estrogen) replacement for up to eighteen months. (b) These rats will also be used to observe general *Brca2*-related pathological changes. **Aim 2:** *Brca2* homozygous knockouts will be characterized on a cellular level. This will include: (a) evaluating cells for truncated *Brca2* protein; (b) testing for the interaction of the truncated *Brca2* protein with RAD51; (c) for nuclear co-localization; and (d) testing the sensitivity of primary embryonic fibroblasts to ionizing radiation. **Aim 3:** Test the hypothesis that the modifying effect of the *Brca2* truncation mutation on *in vivo* radiation sensitivity is organ specific. We will compare the radiation sensitivity of the *Brca2* homozygous knockouts to wild-type littermates (WF strain) for three organs – mammary, thyroid, and liver, using a limiting dilution transplantation/regrowth assay.

Aim 1. The goal of this aim is to determine if mammary carcinomas would develop in *Brca2*$^{-/-}$ rats. We continued to devote all of our efforts in the past year toward developing a model for mammary carcinogenesis.

Maintain rat colonies and expand *Brca2*-SD and *Brca2*-WF knockout rat lines. Currently, the SD line is in the N15 backcross generation. Heterozygous male carriers are being transferred to a repository, so that they will be available to other investigators. The WF line has been discontinued, as efforts to establish a mammary carcinogenesis model in this strain have not been successful.

Conduct short-term mammary bio-assays of hormonal transplantation assays. In 2005, we reported the effects of short-term estrogen replacement given via Silastic capsules on the *Brca2*$^{-/-}$ mammary gland.

Conduct long-term mammary carcinogenesis experiment. The results of long-term analysis for spontaneous tumor development in the SD strain were reported in 2005. These findings have been published (2).

Long-term phenotype in male *Brca2*$^{-/-}$ rats having the WF genetic background. Since the key findings of long-term phenotypic analyses of the SD strain were a high incidence of cataracts and sarcoma in both male and female rats, we assessed 8 male *Brca2*$^{-/-}$ rats having the WF genetic background for the presence of cataracts or spontaneous tumor development. Rats were kept for 12-15 months. Three rats were euthanized due to dental abscesses and three because of respiratory or other illness. The two remaining rats appeared healthy at the conclusion of the study. None of the rats had cataracts or tumors. The resistance of the WF strain to these diseases is likely due to genetic modifiers.

Mammary carcinogenesis studies using chemical carcinogens in rats having the SD genetic background. The results of 6 months of estrogen replacement on mammary tumorigenesis in ovariectomized *Brca2*$^{-/-}$, *Brca2*$^{+/-}$ and *Brca2*$^{+/+}$ SD rats were reported in 2006. Due to complications observed in this model, we explored an alternative to establish a breast cancer model using the chemical carcinogens, 7,12,dimethylbenz(a)anthracene (DMBA) and nitrosomethylurea (NMU). For these analyses, we compared susceptibility of *Brca2*$^{+/+}$ to *Brca2*$^{+/-}$ rats, since it is likely that the small size of *Brca2*$^{-/-}$ rats would compromise survivability. Rats were necropsied 12 or 15 weeks following DMBA or NMU administration, respectively.

Administration of DMBA or NMU did not significantly increase the number of mammary carcinomas in *Brca2*$^{+/-}$ rats having the SD genetic background, compared with those having wild type *Brca2* (Figures 1 and 2). The average number of carcinomas per rat following DMBA treatment was 2.4 +/- 1.9 in wild type rats (n = 24), compared with 3.0 +/- 2.4 (standard deviation) in heterozygotes (n = 25). Similarly, NMU treatment resulted in an average of 2.2 +/- 1.7 carcinomas per rat in *Brca2*$^{+/+}$ animals (n = 23) and 3.2 +/- 2.4 carcinomas per rat in *Brca2*$^{+/-}$ animals (n = 27).

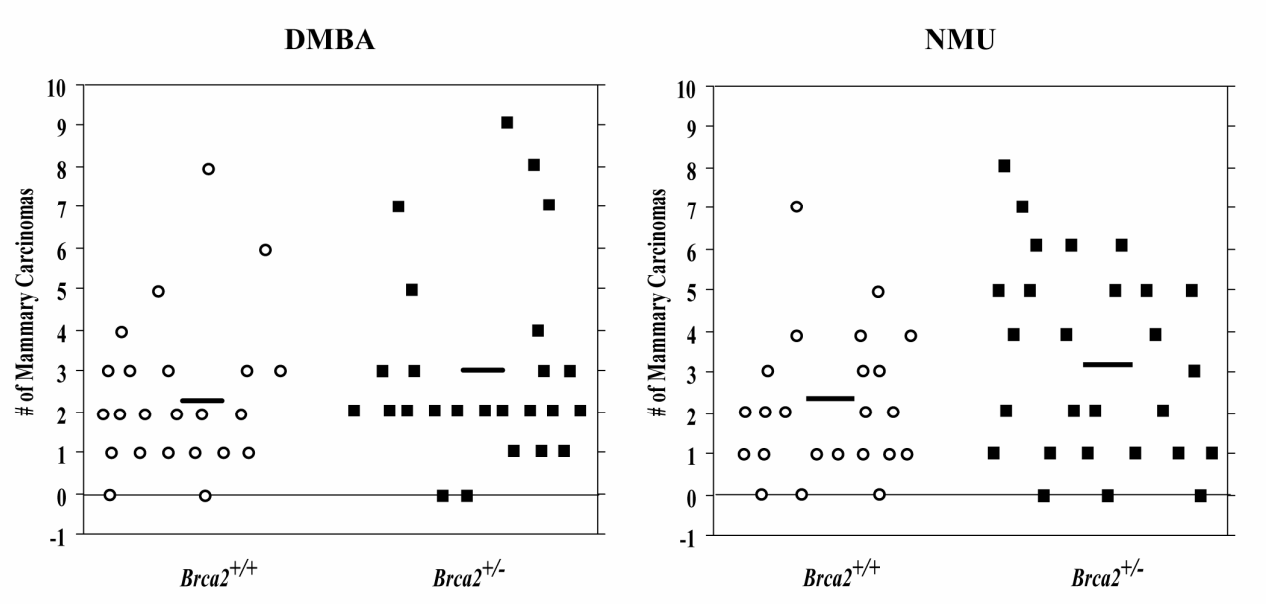

Figure 1. Scatter plots showing the distribution of the individual number of mammary carcinomas in *Brca2*$^{+/+}$ and *Brca2*$^{+/-}$ SD rats treated with DMBA (left panel) or NMU (right panel). Rats were given 65 mg/kg body weight DMBA or 50 mg/kg body weight NMU by gavage at 50-55 days of age and sacrificed 12 or 15 weeks after treatment, respectively. The black horizontal bars represent the mean for each group; each symbol represents the number of mammary carcinomas for each individual rat. ○ = *Brca2*$^{+/+}$, ■ = *Brca2*$^{+/-}$.

Although treatment with either carcinogen did not result in a significant increase in the number of mammary carcinomas in heterozygous rats compared with wild type littermates, NMU-treated heterozygous rats had a slight trend toward increased mammary carcinoma multiplicity (Figure 1). We conclude that the outbred SD genetic background may have contributed to variability in the response to NMU.

Mammary carcinogenesis studies in rats having the WF genetic background. Since a trend toward increased mammary carcinogenesis was seen in SD *Brca2*$^{+/-}$ rats, we conducted a small mammary carcinogenesis study using NMU in *Brca2*$^{+/+}$ (n = 15) and *Brca2*$^{+/-}$ (n = 9) rats having the WF genetic background. The average number of mammary carcinomas in *Brca2*$^{+/+}$ rats was 4.7 +/- 2.5 (standard deviation) and was *Brca2*$^{+/-}$ 5.3 +/- 2.9. There was no statistical difference between these groups (t test, StatView, SAS, Cary, NC).

Ovarian transplant studies. The goal of this model was to correct insufficient ovarian hormone secretion in *Brca2*$^{-/-}$ recipients by transplanting *Brca2*$^{+/+}$ ovaries.

In 2006, we reported the results of short term ovarian transplant studies. We showed that transplantation of *Brca2*$^{+/+}$ ovaries into the subscapular fat pad of *Brca2*$^{-/-}$ recipients was successful, as determined by estrus cycling and a growth response in the *Brca2*$^{-/-}$ mammary gland, and by verification of the presence of ovarian tissue by histology of excised transplant sites.

We assessed mammary carcinogenesis over a 9- to 12-month period in 12 controls (*Brca2*$^{+/+}$ donor ovary transplanted into *Brca2*$^{+/+}$ recipients) and in 20 *Brca2*$^{-/-}$ rats that received

Brca2$^{+/+}$ ovaries. Neither group had mammary carcinomas at the conclusion of the experiment. We surmise that the transplanted ovaries stopped production of estrogen over time, based on the appearance of the transplanted ovarian tissue at the conclusion of the experiment. In the majority of rats, the transplanted ovary was cystic and/or necrotic.

Mammary transplant studies. The goal of these studies was to assess carcinogenesis of the *Brca2*$^{-/-}$ mammary gland after allowing it to develop in the normal hormonal environment of *Brca2*$^{+/+}$ hosts.

In the 2006 report, we discussed validation of the mammary gland transplant methodology following assessment of short term transplants. We have concluded a long-term mammary carcinogenesis experiment using 12 controls (*Brca2*$^{+/+}$ mammary gland transplanted into *Brca2*$^{+/+}$ hosts) and 20 *Brca2*$^{+/+}$ recipients having *Brca2*$^{-/-}$ transplants. Rats were kept for 12 months in order to assess for tumor formation in the transplanted tissue. At necropsy, the susbscapular fat pad was dissected from 8 controls and 17 *Brca2*$^{-/-}$donors, fixed in 10% neutral buffered formalin, and stained with aluminum carmine for whole mount analysis. Some of the formalin-fixed samples (6 controls and 11 from *Brca2*$^{-/-}$donors) were embedded in paraffin for analysis of histology from hematoxylin and eosin (H&E) stained sections. Some samples were split for both whole mount and histology (3 controls and 9 from *Brca2*$^{-/-}$donors). The results of evaluation of H&E stained sections are summarized in Table 1.

Table 1. Analysis of histology of transplanted mammary tissue from sections.

Donor→Recipient *Brca2* Genotype	**Histologic Appearance of Transplanted Mammary Tissue**			
	Normal	**Normal with Hyperlobular Areas**	**Milk Cyst**	**Carcinoma**
Brca2$^{+/+}$→*Brca2*$^{+/+}$	4/6	0/6	1/6	1/6
Brca2$^{-/-}$ →*Brca2*$^{+/+}$	6/11	3/11	1/11	0/11

Normal mammary ducts were the most common finding seen in histologic sections of tissue (Table 1 and Figure 2A). This was true for transplants from both *Brca2* genotypes. However, 3 out of 11 slides evaluated from *Brca2*$^{-/-}$ donor transplants had proliferative hyperlobular foci, in addition to normal areas. Milk cysts were observed in two transplants, one from each donor genotype (Figure 2B). The only carcinoma found originated from a *Brca2*$^{+/+}$ transplant (Figure 2C).

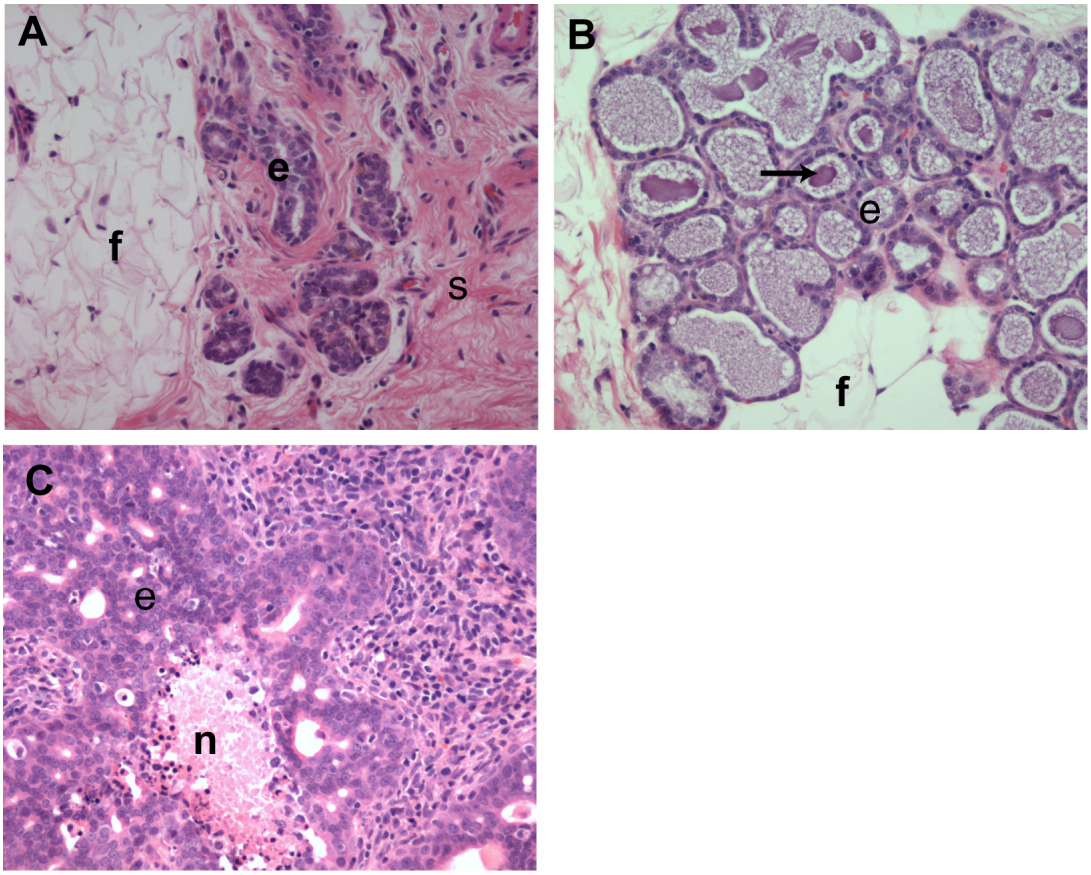

Figure 2. Hematoxylin and eosin stained sections showing histologic appearance of mammary tissue transplanted into subscapular fat pads of *Brca2*$^{+/+}$ recipients. Tissue was removed 1 year after surgical transplantation. **f** = fat cells, **e** = epithelium, **s** = stroma, **n** = necrosis. Panel A: transplanted epithelium from *Brca2*$^{+/+}$ donor a having a normal appearance. Panel B: Transplant from a *Brca2*$^{-/-}$ donor having a milk cyst. The arrow points to a dilated duct containing caseinous material. Panel C: Mammary carcinoma from *Brca2*$^{+/+}$ donor having a necrotic center. Photographs were taken at 20X magnification.

The results of morphologic assessment of whole mounted transplant tissue are summarized in Table 2. The majority of controls having *Brca2*$^{+/+}$ transplants had a low degree of branching and lobularity (Figure 3A). In contrast, *Brca2*$^{-/-}$ transplants had a higher percentage of those with a proliferative phenotype, with a high degree of branching and/or lobularity (Figure 3B). The hyperlobular appearance may therefore coincide with or precede the presence of caseinous milk cysts.

We conclude that the mammary transplant methodology was appropriate, as one carcinoma developed spontaneously from a *Brca2*$^{+/+}$ donor. This finding coincides with the rare incidence of spontaneous mammary carcinomas in WF rats. The high degree of lobularity in the *Brca2*$^{-/-}$, compared with *Brca2*$^{+/+}$ transplants, may indicate an increased sensitivity to prolactin or progesterone, as these hormones play a major role in lobular growth and differentiation.

Table 2. Morphologic analysis of transplanted tissue morphology from whole mounts.

Donor→Recipient *Brca2* Genotype	**Degree of Branching**			**Degree of Lobularity**	
	Low	**High**	**Both**	**Low**	**High**
$Brca2^{+/+} \rightarrow Brca2^{+/+}$	7/8	0/8	1/8	8/8	0/8
$Brca2^{-/-} \rightarrow Brca2^{+/+}$	8/17	6/17	3/17	9/17	8/17

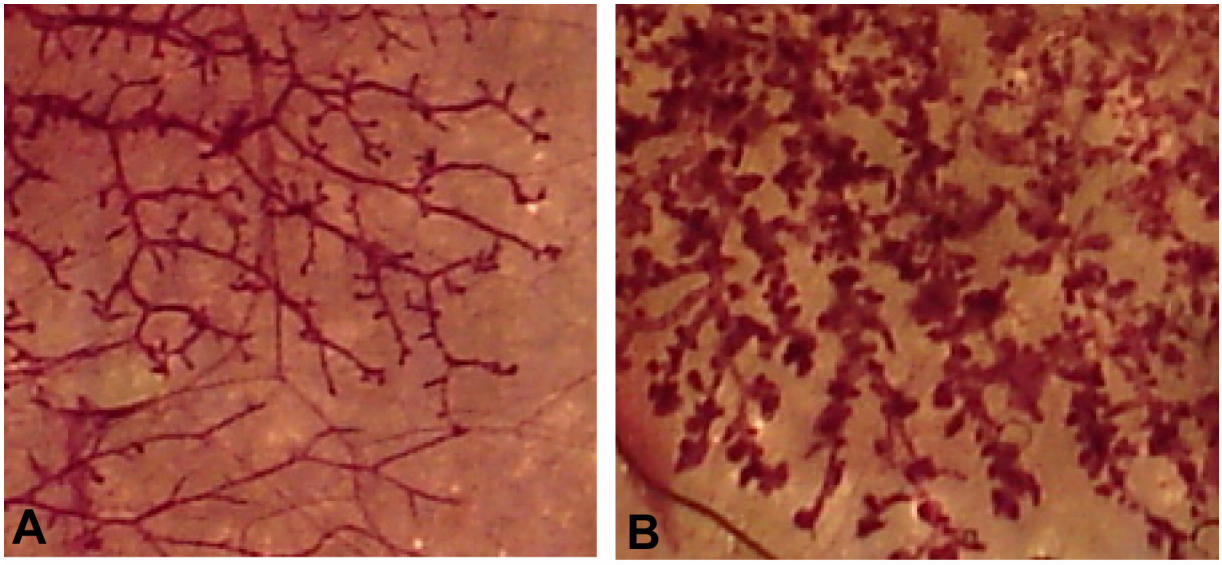

Figure 3. Aluminum carmine stained whole mounts of transplanted mammary tissue from A: $Brca2^{+/+}$ donor, showing minimal branching and lobularity; and B: $Brca2^{-/-}$ donor, showing a high degree of branching and lobularity. Photos were taken with a digital camera.

Aim 2. Characterization of *Brca2* homozygous knockouts

Assay for the presence of truncated *Brca2* in knockout mammary cells. In 2006, we reported the presence of full length BRCA2 in $Brca2^{+/+}$ and $Brca2^{+/-}$ testes extracts using western blotting. The protein was absent in the testes extracts of $Brca2^{-/-}$ rats. A truncated form was present in $Brca2^{-/-}$ and $Brca2^{+/-}$ extracts, but was absent in $Brca2^{+/+}$ samples. These findings were subsequently published in (Cotroneo, et al., 2006). We did not detect the BRCA2 protein in mammary gland extracts, due to low expression levels.

Assay for the interaction of the truncated BRCA2 protein and RAD51 and determine their cellular localization. Due to undetectable expression levels of BRCA2 in the mammary gland using the available antisera (from L. Chodosh), we did not conduct these assays.

Aim 3. Determine the *in situ* radiation sensitivity for mammary, thyroid, and liver parenchymal clonogenic (stem-like)cells using a limiting dilution transplantation assay *in vivo*. We did not pursue this Aim, as all of our resources were devoted to developing a mammary carcinogenesis model.

KEY RESEARCH ACCOMPLISHMENTS

-We evaluated mammary carcinogenesis in *Brca2*$^{+/-}$ rats having SD background genetics using the chemical carcinogens DMBA and NMU. Heterozygous rats did not have significantly increased mammary tumorigenesis, compared with control littermates having wild type *Brca2*, although NMU-treated *Brca2*$^{+/-}$ rats had a slight increase in the number of mammary carcinomas. Administration of NMU to *Brca2*$^{+/-}$ rats having the WF genetic background did not result in increased tumorigenesis, compared with wild type controls.

-We concluded a long-term study evaluating an ovarian transplant model, where *Brca2*$^{+/+}$ donor ovaries were given to *Brca2*$^{-/-}$ recipients in order to correct ovarian hormone secretion. Mammary carcinomas did not develop, presumably due to limited long term survival of the transplants.

-We completed long-term analysis for mammary carcinogenesis in *Brca2*$^{+/+}$ hosts receiving *Brca2*$^{+/+}$ or *Brca2*$^{-/-}$ mammary transplants. The *Brca2*$^{-/-}$ mammary glands did not develop into carcinomas. However, they showed a higher frequency of hyperlobularity, compared with *Brca2*$^{+/+}$ transplanted mammary glands, suggesting that the absence of BRCA2 may result in increased hormonal sensitivity.

REPORTABLE OUTCOMES

Our paper describing the phenotypic analysis of the *Brca2* knockout rat has been published (2).

The results of the chemical carcinogenesis and transplant studies have been included in a review article entitled "Genetically Engineered Rat Models for Breast Cancer", for publication in *Breast Disease* (3). The article is attached (see Appendix).

CONCLUSIONS

We showed that our rat *Brca2* knockout allele codes for a truncated protein which lacks most of the peptide coded from exon 11 to the carboxy-terminus. We demonstrated that rats homozygous for this knockout allele develop cataracts and a variety of cancers over their first year of life. Unexpectedly, none of these excess cancers were of breast origin. The likely explanation for this is the observation that female germ cells (ova) do not normally develop. This is likely due to defective homologous recombination downstream from *Brca2* inactivation. The lack of developing follicles reduces circulating estrogen levels. The lack of physiologic estrogen levels likely prevents mammary carcinoma development.

To circumvent this problem, we used several methods. We evaluated estrogen replacement using surgically implanted capsules, but this study was dropped due to toxicity. Alternatively, we attempted to provide a normal hormonal environment for the *Brca2*$^{-/-}$ mammary gland by developing two tissue transplant models. Using rats having the WF genetic background, we transplanted *Brca2*$^{+/+}$ ovaries into *Brca2*$^{-/-}$ recipients. Although the transplanted ovaries induced estrus cycling in the recipients initially, no mammary carcinomas developed, presumably due to lack of long-term survival of the ovarian tissue. As an alternate strategy,

Brca2$^{-/-}$ mammary glands were transplanted into *Brca2*$^{+/+}$ recipients. Although the *Brca2*$^{-/-}$ transplants showed a higher degree of lobularity and branching compared to controls, they did not develop into carcinomas. As an additional strategy to develop a mammary carcinogenesis model, we induced mammary carcinomas chemically with NMU and DMBA in *Brca2*$^{+/-}$ and *Brca2*$^{+/+}$ rats. However, incidence did not differ between these groups.

Although our attempts to establish a mammary cancer model using the *Brca2*$^{-/-}$ knockout rat were unsuccessful, we have produced a valuable genetic model. This model provides an important alterative to traditional mouse *Brca2* knockouts, due to the viability of *Brca2*$^{-/-}$ offspring. Therefore, further studies can be done to study the functions of the Brca2 protein in various tissues, and their relationship to cancer. Additionally, the *Brca2*$^{-/-}$ had an unexpected, highly penetrant phenotype of increased cataractogenesis, providing a model for the study of this disease.

REFERENCES

1. Zan, Y., Haag, J.D., Chen, K.S., Shepel, L.A., Wigington, D., Wang, Y.R., Hu, R., Lopez-Guajardo, C.C., Brose, H.L., Porter, K.I., Leonard, R.A., Hitt, A.A., Schommer, S.L., Elegbede, A.F., and Gould, M.N. Production of knockout rats using ENU mutagenesis and a yeast-based screening assay. *Nat. Biotechnol.,* 21(6): 645-651, 2003.

2. Cotroneo, M.S., Haag, J.D., Zan, Y., Lopez, C.C., Thuwajit, P., Petukhova, G.V., Camerini-Otero, R.D., Gendron-Fitzpatrick, A., Griep, A.E., Murphy, C.J., Dubielzig, R.R., and Gould, M.N. Characterizing a rat *Brca2* knockout model. *Oncogene*, 26(11): 1626-1635, 2007.

3. Smits, B.M., Cotroneo, M.S., and Gould, M.N. Genetically engineered rat models for breast cancer. Invited review, submitted.

APPENDIX

Zan, Y., Haag, J.D., Chen, K.S., Shepel, L.A., Wigington, D., Wang, Y.R., Hu, R., Lopez-Guajardo, C.C., Brose, H.L., Porter, K.I., Leonard, R.A., Hitt, A.A., Schommer, S.L., Elegbede, A.F., and Gould, M.N. Production of knockout rats using ENU mutagenesis and a yeast-based screening assay. *Nat. Biotechnol.,* 21(6): 645-651, 2003.

Cotroneo, M.S., Haag, J.D., Zan, Y., Lopez, C.C., Thuwajit, P., Petukhova, G.V., Camerini-Otero, R.D., Gendron-Fitzpatrick, A., Griep, A.E., Murphy, C.J., Dubielzig, R.R., and Gould, M.N. Characterizing a rat *Brca2* knockout model. *Oncogene*, 26(11): 1626-1635, 2007.

Smits, B.M., Cotroneo, M.S., and Gould, M.N. Genetically engineered rat models for breast cancer. Invited review, submitted.

nature biotechnology

Production of knockout rats using ENU mutagenesis and a yeast-based screening assay

Yunhong Zan[1,2], Jill D Haag[1,2], Kai-Shun Chen[1], Laurie A Shepel[1], Don Wigington[1], Yu-Rong Wang[1], Rong Hu[1], Christine C Lopez-Guajardo[1], Heidi L Brose[1], Katherine I Porter[1], Rachel A Leonard[1], Andrew A Hitt[1], Stacy L Schommer[1], Anu F Elegbede[1] & Michael N Gould[1]

The rat is a widely used model in biomedical research and is often the preferred rodent model in many areas of physiological and pathobiological research. Although many genetic tools are available for the rat, methods to produce gene-disrupted knockout rats are greatly needed. In this study, we developed protocols for creating N-ethyl-N-nitrosourea (ENU)-induced germline mutations in several rat strains. F_1 preweanling pups from mutagenized Sprague Dawley (SD) male rats were then screened for functional mutations in *Brca1* and *Brca2* using a yeast gap-repair, *ADE2*-reporter truncation assay. We produced knockout rats for each of these two breast cancer suppressor genes.

The rat is an important murine model for studies in physiology, pathobiology, toxicology, neurobiology and a variety of other disciplines[1]. The rat is of value in these fields because it is larger than the mouse and because a plethora of organ-specific physiologic and disease models have been developed for it over the last century. The importance of the rat as a biological model has led to an intense effort to also establish it as a strong genetic model. A key genetic technology available for the mouse but not for the rat is the production of animals in which specified genes have been disrupted (knockout animals)[1]. This is due in part to the inability to produce functional rat embryonic stem cells. In addition, rats have not been generated to date by nuclear transfer (National Institutes of Health Meeting on Rat Model Priorities, May, 1999, http://www.nhlbi.nih.gov/resources/docs/gpg.htm). Here we report a method to produce knockout rats using an alternative approach.

The first step of our method consists of mutagenizing male rats with ENU. In mice, ENU is currently the mutagen of choice for the production of heritable altered phenotypes[2,3]. ENU was the most efficient mutagen tested[4] and was estimated to cause one functional mutation per 1,000 alleles tested (0.5–1.5 mutations per locus per progeny)[2,3]. It is important to stress the word 'functional' because the total number of mutations is much higher. Beier et *al.* calculated that theoretically there would be 10 actual sequence changes per 1,000 alleles, but that only 1 in 10 of these would result in a functional change leading to a phenotypic variant[5]. A main goal in this study was to develop a method that not only identifies F_1 rats with mutations in selected genes, but also prequalifies mutations that are likely to alter function, thus reducing wasted effort in downstream characterization of mutations that do not alter gene function. Thus, the second step of our approach involves yeast-based screening assays that select for various classes of functional mutations. These assays use gap-repair cloning to integrate either genomic DNA (gDNA) or cDNA of a selected gene between the yeast promoter ADH1 and the reporter gene *ADE2* to form a chimeric protein. If the DNA from a specific allele contains functional mutations that interfere with translation, then an active ADE2 chimeric protein is not produced, resulting in small, red yeast colonies instead of the large, white colonies found when screening wild-type DNA. We have combined ENU mutagenesis and yeast-based screening assays to generate two knockout rats for the breast cancer suppressor genes *Brca1* and *Brca2*.

RESULTS

Development of ENU mutagenesis protocols for the rat

Genome-wide mutagenesis protocols using ENU were established for three rat strains: inbred Wistar-Furth (WF), inbred Fischer 344 (F344) and outbred SD. Sexually mature 9-week-old male rats were given either a single intraperitoneal injection of ENU or a split dose with injections spaced a week apart. Fertility was determined at various times after ENU treatment (Table 1). The strains differed in their sensitivity to ENU-induced permanent sterility in a dose-dependent manner, with the WF strain being the most sensitive and the SD strain able to tolerate the highest doses. In all strains tested, ENU-treated male rats rarely recovered fertility after a period of complete sterility, unlike many strains of ENU-treated mice[6]. Average litter size was reduced in both the SD and F344 strains around weeks 7–9 after ENU treatment, the same time period in which we observed reduced fertility in the ENU-treated males. All fertile mutagenized male rats provided viable litters up to 1 year after ENU treatment; however, their lifespan was shortened, with many developing skin and kidney tumors and lymphomas at approximately 1 year of age. None of the doses listed in Table 1 were acutely toxic to the rat strains tested.

Mutagenized male rats were used to generate F_1 offspring, and phenotypically variant mutant pups were visually identified before weaning at 3–4 weeks of age. Abnormalities of the eyes, tail and growth were

[1]Department of Oncology, McArdle Laboratory for Cancer Research, 1400 University Avenue, University of Wisconsin–Madison, Madison, Wisconsin 53706, USA. [2]These authors contributed equally to this work. Correspondence should be addressed to M.N.G. (gould@oncology.wisc.edu).

Table 1 Effects of ENU treatment on male rat fertility and determination of heritable, phenotypic mutations of F_1 rats derived from ENU-treated male rats

Rat strain	ENU dose (mg/kg)	% male rats fertile[a]	No. phenotypic mutants observed[b]	Heritable	Non-heritable	Sterile	Unknown[c]
SD	75	100%	nd				
SD	100	80%	511068	0	1	0	4
SD	120	33%	21347	0	1	0	1
SD	150	0%	nd				
SD	200	0%	nd				
SD	2 × 50	100%	4/524	1	2	0	1
SD	2 × 60	100%	7414758	13	8	4	49
SD	2 × 75	20%	11112	0	0	0	1
SD	2 × 100	0%	nd				
SD	0	100%	31849	0	0	2	1
F344	75	100%	nd				
F344	100	67%	161587	1	1	5	9
F344	120	0%	nd				
F344	2 × 50	60%	151297	1	1	1	12
F344	2 × 60	40%	51145	0	0	0	5
F344	2 × 75	0%	nd				
F344	2 × 100	0%	nd				
F344	0	100%	2/372	0	0	0	2
WF	25	30%	31366	1	1	0	1
WF	35	33%	1136	0	1	0	0
WF	50	25%	2125	0	0	0	2
WF	75	0%	nd				
WF	100	0%	nd				
WF	2 × 15	17%	nd				
WF	2 × 25	17%	2128	0	0		1
WF	2 × 50	0%	nd				
WF	2 × 75	0%	nd				
WF	0	100%	0151	nla	nla	nla	nla

[a]ENU-treated male rats (n = 3–12) were paired with fertile female rats every 2 weeks from weeks 7–26 after ENU administration. Vaginal plugs were observed for all infertile breeding pairs. Fertility was based upon ability to produce a viable litter when bred with females of the same strain. [b]All F_1 pups from litters conceived at least 10 weeks after ENU treatment were visually examined for gross abnormalities in physical development or behavior at least twice before weaning at approximately 21 d of age. Details of the mutants are given in Supplementary Table 1 online. nd, not determined; n/a, not applicable. [c]Includes all phenotypic mutant F_1 rats that were not evaluated or that died before producing a litter.

those most commonly observed in the F_1 pups (see Supplementary Table 1 online). Using a split dose protocol of 2 × 60 mg ENU/kg body weight in SD male rats, a screen of visually apparent phenotypes revealed a rate of phenotypically detectable mutants of 1 in 64 F_1 rats (Table 1 and Supplementary Table 1 online). A subset of the phenotypic mutant F_1 rats was tested for inheritance. Approximately one-half of those that produced viable litters showed heritability of the trait (Tables 1 and 2 and Fig. 1).

Development of a yeast-based assay for mutation screening

We chose to use the outbred SD rat for the mutation-screening studies owing to its tolerance of ENU treatment, to the variety of ENU-induced, heritable phenotypic mutants identified and to its large litter sizes. We used a split dose of ENU (2 × 60 mg/kg) to mutagenize male SD rats. These rats were then bred to wild-type female SD rats to produce F_1 pups that were screened for mutant alleles of *Brca1* and *Brca2*.

Two related truncation assays[7].* were developed to screen the *Brca1* and *Brca2* genes of these F_1 pups for functional mutations that could interfere with protein translation (Fig. 2). The first assay uses gDNA as a starting macromolecule, whereas the second assay begins with total RNA that is reverse-transcribed to cDNA. In both assays, PCR is used to amplify fragments of the gDNA exon or the cDNA targeted for knockout (Fig. 2). The gap-repair vectors are customized for each targeted fragment by cloning in small 5′ and 3′ sequences from the fragment of interest. For *Brca1*, three vectors were generated, and the third vector (used for the cDNA assay) is shown in Fig. 2. For *Brca2*, three vectors were also generated and the second is shown in Fig. 2. The 5′ and 3′ end sequences from each fragment were cloned in tandem and separated by a unique *Sma*I restriction enzyme site, which allows the plasmid to be linearized. The linearized vector is then transformed together with unpurified PCR product of the gene-specific fragment into competent yeast (*S. cerevisiae*, yIG397 strain) cells. Following transformation, the gene-specific fragment is cloned *in vivo* into the gap-repair vector by homologous recombination. Once incorporated into the vector, the gene fragment is then located behind the yeast promoter *ADH1* and in front of the reporter gene *ADE2*, with which it jointly codes for a functional chimeric protein. This yeast strain lacks ADE2 function that can be restored by this chimeric protein. Yeast cells that produce chimeric ADE2 protein grow efficiently and form large white colonies when plated on selective medium. In the absence

Table 2 ENU-induced heritable phenotypes

Line	Strain	F_1 founder sex	Initial ENU dose (mg/kg)	Observed phenotype	Confirmed in multiple litters
9	F344	Female	100	No left eye	Yes
18	SD	Female	2 x 60	Crooked tail and slit eyes	Yes
19	SD	Male	2 x 50	Growth on tail[a]	Yes
28	SD	Female	2 x 60	Red ring eyes[a]	Yes
29	SD	Female	2 x 60	Oblong face	Yes
32	SD	Female	2 x 60	Slit eyes[a]	Yes
38	SD	Male	2 x 60	Curved tail	Yes
42	SD	Female	2 x 60	Bald spots	Yes
44	F344	Female	2 x 50	Hooklike tail[a]	Yes
54	SD	Female	2 x 60	Scaly skin	Yes
56	WF	Female	25	Head tilt	Yes
60	SD	Female	2 x 60	Scaly skin	Yes
61	SD	Male	2 x 60	Swollen feet	Yes
63	SD	Male	2 x 60	Additional digits on hind feet[a]	Yes
64	SD	Male	2 x 60	Additional digits on hind feet	Yes
68	SD	Male	2 x 60	Kinked tail	No[b]
71	SD	Male	2 x 60	Curly hair and whiskers[a]	No[b]

[a]Observed altered phenotypes are shown in Figure 1. [b]Only one litter has been produced to date; however, breeding of founder rat is ongoing.

of functional chimeric protein the yeast cells grow poorly and form small red colonies. Thus, for *Brcal* and *Brca2*, if the DNA donor F_1 pup is wild type for the incorporated gene fragment, the assay yields large white colonies. If, however, the donor rat DNA contains a functional mutation in one allele of *Brcal* or *Brca2* in the assayed fragment, the translation of a functional hybrid ADE2 protein is prevented and small red colonies are produced. In this assay, a functional mutation for *Brcal* and *Brca2* in a rat will be heterozygous; therefore, approximately half the colonies will be red and half white after accounting for a background rate of red colonies.

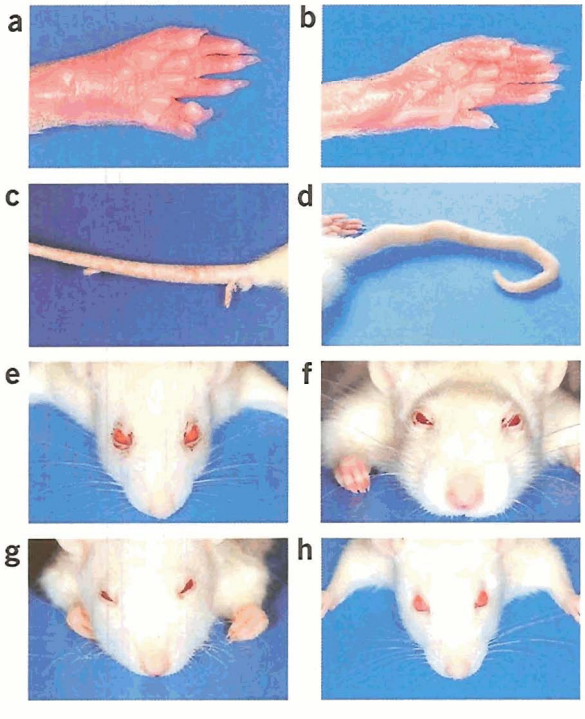

Figure 1 Heritable phenotypic mutant rats. Male rats were given ENU and then bred to produce F_1 pups that were observed for visible altered phenotypes. Details of these derivations are listed in Table 2. The phenotypic mutants and control rats shown include: (a) line 63 rat with multiple digits on hind foot; (b) control rat hind foot; (c) line 19 rat with growths on tail; (d) line 44 rat with hook-like tail; (e) line 28 rat with red ring eyes; (f) line 32 rat with slit eyes; (g) line 71 rat with curly hair and whiskers, no eye abnormality; (h) control rat.

Establishment of a *Brca2* knockout rat line

We looked for disruption of the *Brca2* gene with a gDNA assay, focusing on exon 11 (the largest exon, representing roughly half of the cDNA) (Fig. 2). This large exon was divided into three regions of ~1,700 base pairs (bp) each, and the second and third fragments were used for screening. Primer sequences for each fragment are given in Supplementary Table 2 online. We screened gDNA from 788 preweanling F_1 rat pups before finding a mutated *Brca2* allele using the second-fragment vector (Fig. 2). The knockout rat was the only one identified with this *Brca2* mutation out of 296 F_1 offspring screened from this specific mutagenized father, indicating that this mutation was not a preexisting germline mutation in this SD father. Similarly, the female parent produced over 40 offspring, including 10 littermates of the knockout rat, none of which carried the *Brca2* mutation. The *Brca2* knockout rat was detected in our gDNA assay by a yeast plate that had approximately 45% red colonies and 55% white colonies (Fig. 3a, right dish). The average background of red colonies was very low (Fig. 3a, left dish) for this gDNA assay (0.5% ± 0.6%, n = 10). Next, individual red and white yeast colonies were sequenced. A nonsense transversion mutation was detected at nucleotide T4254 of the *Brca2* cDNA that converted TAT (tyrosine) to TAA (stop codon) at Tyr1359 (Fig. 3a, lower panel, upper and center sequences). A/T→T/A transversion mutations are the most common mutation type (44%) found in mice bearing ENU-induced, phenotypically detectable germline mutations[2,3]. Genomic DNA from the founder rat 3983 was sequenced and found to contain the identical mutation as detected in the yeast red colonies (Fig. 3a, lower panel, lower sequence).

In conjunction with the gDNA assay, we used the cDNA yeast assay with the same *Brca2* fragment 2 vector to screen N_2 pups resulting from the breeding of the *Brca2* knockout founder male rat 3983 to SD females. Both methods identified the same 9 out of 14 pups from the first litter of rats carrying this *Brca2* mutation, and these results were confirmed by the direct sequencing of gDNA from each N_2 pup. This verified the utility of the yeast assay starting from either gDNA or RNA. This cDNA assay had a background of 15.3% ± 2.0% (n = 20) for wild-type pups and 48.5% ± 2.1% (n = 36) red colonies for knockout pups. Sequencing *Brca2* fragment 2 DNA of 60 red colonies from the cDNA assay of the knockout pups confirmed this background frequency, in that 17% (10160) of the sequenced clone fragments lacked the specific stop codon mutation. Interestingly, the

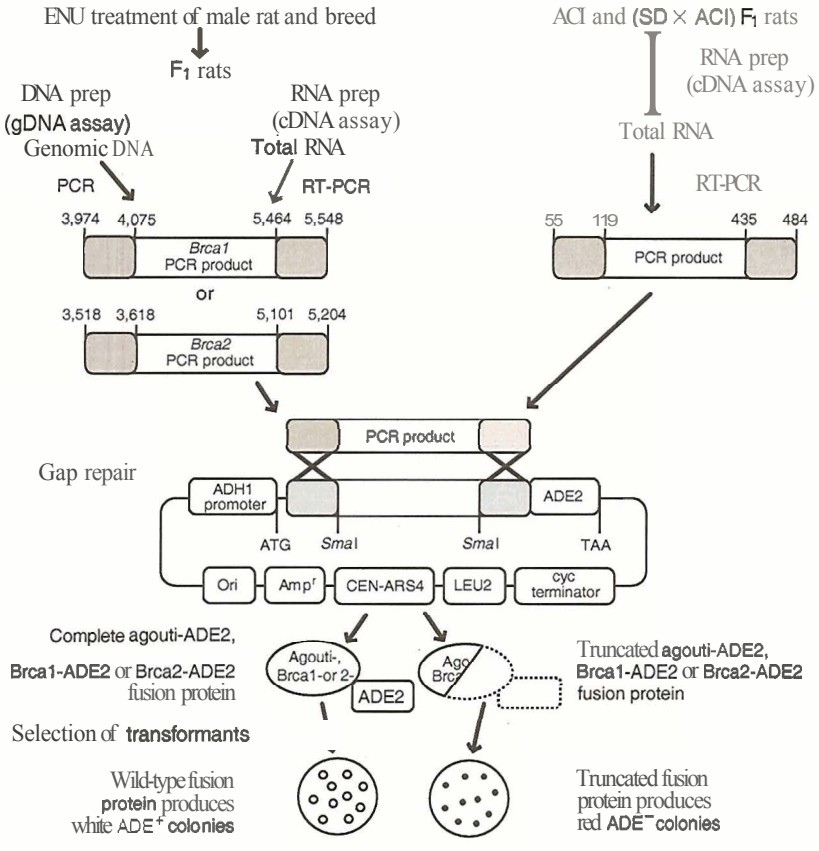

Figure 2 Brcal, *Brca2* and *agouti* yeast cDNA/gDNA truncation assays. For Brcal and *Brca2* assays, male rats are treated with ENU and bred to produce F_1 pups. DNA and RNA are isolated from tail clipsof one-week-old F_1 rats for Brcal and *Brca2*. For the A (*agouti*) assays, a small piece of ventral skin from ACI or (SD x ACI) F_1 rats is excised and used for RNA isolation. Total RNA is reverse-transcribed and both the resultant cDNA (Brcal or *A*) and isolated gDNA (*Brca2*) are amplified using PCR for selected DNA regions. The gap repair vectors are customized for each targeted fragment. The 5' and 3' sequences for the Brcal vector are derived from nucleotides 3974–4075 and 5464–5548 of the *Brca1* cDNA (GenBank no. AF036760), respectively. The 5' and 3' sequences for the *Brca2* vector are derived from nucleotides 3518–3618 and 5101–5204 of the *Brca2* cDNA (GenBank no. U89653, mRNA), respectively. The Brcal and *Brca2* vectors shown are those that ultimately led to the identification of the knockouts. A single gap vector was constructed using the 5' and 3' sequences derived from nucleotides 55–119 and 435–484 of the A mRNA sequence (GenBank no. AB045587), respectively. Following transformation, the gene-specific fragment is cloned *in* vivo into the gaprepair vector by homologous recombination. The wild-type gene fragment codes for a functional fusion protein with the *ADE2* gene of the vector and forms large white colonies when plated. A truncated gene fragment will not form a functional protein and the colonies will be small and red.

background rate for the cDNA assay was over an order of magnitude higher than the gDNA assay, suggesting that most of the background in the cDNA assay comes from DNA replication errors in the reverse transcription reaction.

N_2 pups produced from founder 3983 included 35 heterozygous knockouts out of 64 pups, demonstrating the mendelian inheritance of this knockout gene. *Brca2* heterozygous N_2 male and female rats were bred to produce *Brca2* homozygous knockout pups. The ratio of *Brca2* homozygous knockout rats to *Brca2* heterozygous rats to wild-type rats was approximately 1:2:1. Body weight data were collected for all N_2F_2 pups starting at weaning. The results illustrate a clear phenotype of growth inhibition of male and female *Brca2* homozygous knockout rats (Fig. 3b). These rats are sterile and reduced in size but otherwise healthy. Histopathological analysis of gonads from the *Brca2* homozygous rats shows severe atrophy that is not observed in the *Brca2* heterozygous and wild-type rat gonads (Supplementary Fig. 1 online).

Production of a Brcal mutant rat line

Customized gap-repair vectors for screening *Brcal* (Fig. 2) consisted of two gDNA vectors targeting exon 11 (the largest exon, target fragments 1 and 2) and one cDNA vector targeting *Brcal* from the 3' end of exon 11 to the end of the open reading frame (ORF) (fragment 3). Primer sequences for the three fragments are given in Supplementary Table 2 online. After screening 1,965 pups, we identified a *Brcal* mutation in founder rat 5385 using the cDNA assay (Fig. 2). This rat was the only one with this mutation identified in 273 offspring from the same mutagenized SD father and in more than 40 offspring, including 14 littermates, from the SD wild-type mother. The background rate of red colony formation in this assay was 12.2% ± 3.3% (n = 1,485) for wild-type DNA compared to 44.3% in the identified mutant. Haploid DNA from red yeast colonies was sequenced, revealing a complete loss of *Brcal* exon 22 (74 bp) (Fig. 4). We sequenced introns 21 and 22 in search of a splicing mutation to explain the loss of this exon. A T→C mutation was identified within the splicing branch site of intron 21 (TGGTGAT to TGGCGAT) (Fig. 4d,e). A T/A→G/C transition mutation is the second most common type (38%) of ENU-induced mutations[2,3]. The mutation in the branch site of intron 21 caused the splice donor site to skip over exon 22 and find a branch site in intron 22. This led to splicing out of the 74-bp exon 22 and also caused a frameshift downstream from exon 21, exposing a stop codon at the exon 23–24 border (Supplementary Fig. 2 online). Recently, the female founder 5385 has produced two *Brcal* heterozygous rats out of eight pups, demonstrating germline transmission of this mutation.

Nonsense-mediated decay

An anticipated problem using RNA as a starting material for this assay is the potential destruction by cell surveillance mechanisms, such as nonsense-mediated decay (NMD)[9–11], of mRNA transcribed from the mutant allele. We quantified the extent of NMD of the mutated *Brca2* mRNA by comparing the yield of red colonies in the knockout rat samples minus background in the wild-type samples using the cDNA assay (48.5–15.3%) versus the yield of red colonies in the knockouts minus background using the gDNA assay (44.8–0.5%). The same gDNA *Brca2* fragment 2 gap vector was used for both the cDNA and gDNA assays. From these results, NMD is calculated to occur at an approximate rate of [1 – (33/44)] or 25%.

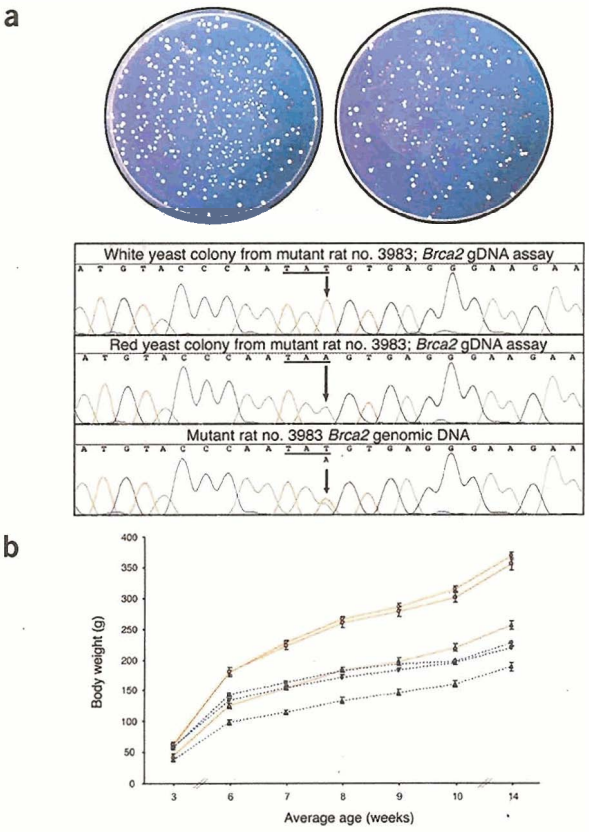

Figure 3 Identification of a *Brca2* knockout rat. (a) Screening for a *Brca2* knockout rat. Yeast cells transformed with gap vector and a PCR product enriched for *Brca2* fragment 2 (nucleotides 3518–5204) were plated on selective medium. When gDNA obtained from a rat (SD) with two wild-type alleles was assayed, the resultant plate contained mostly large white colonies (left dish). In contrast, when the DNA is from a rat in which one allele of *Brca2* was functionally mutated, the resultant colonies were an almost equal mixture of red and white colonies (right dish). Red and white colonies from the plate on the right were picked and used to obtain *Brca2* fragment 2 DNA sequence. The sequence from white yeast colonies (lower panel, upper, representative of four colonies tested) is that of wild-type rat *Brca2*, whereas the sequence from red colonies (lower panel, center, representative of eight colonies tested) has a transversion mutation at T4254 (indicated by the arrow) of the cDNA [TAT (tyrosine)→ TAA (stop)]. Genomic DNA from the heterozygous knockout rat no. 3983 contains both T and A at nucleotide 4254 as seen in the lower sequence (represents two independent tests). The sequences shown in the lower panel span nucleotides 4242–4266 of the rat *Brca2* cDNA. (b) *Brca2* knockout body weight phenotype. Male (solid orange lines) and female (dashed blue lines) *Brca2* homozygous (△), heterozygous (○) knockout rats and wild-type littermates (□) were weighed through their current age of 14 weeks (error bars are ± s.d.).

Because this level of NMD was modest, we challenged our cDNA-based assay using a rat A (also known as *agouti*) locus model in which ~85% of the mutant RNA is subject to NMD[11]. Agouti rat strains such as the ACI rat carry two copies of the wild-type locus, whereas nonagouti rats such as SD carry two identical mutant alleles, each with two truncating mutations in the A gene. We designed a yeast gap vector for this gene that allowed the entire ORF to be cloned *in vivo* in yeast (Fig. 2). We found that our cDNA assay could routinely detect the A mutation in (SD × ACI) F_1 pups, which had 12.4% ± 1.8% (n=52) red colonies, whereas the wild-type ACI group had a background of 4.4% ± 1.6% (n=40) red colonies ($P < 0.0001$, unpaired t-test). NMD was estimated to remove approximately 80% of the RNA coded from the mutated A allele of the F_1 pup, which corresponds well with the above-referenced northern analysis[11]. Note also that the lower background rate of 4.4% red colony formation for the A cDNA assay (500 bp) as compared to that of the Brcal (12.2%, 16 kb) and *Brca2* (15.3%, 17 kb) cDNA assays demonstrates that background is proportional to the size of the gene or gene fragment being screened. A second estimate of background was obtained by sequencing for the A mutation in individual red colonies from a yeast assay of the (SD × ACI) F_1 pups. Of 61 red colonies evaluated, 5 had random mutations, giving a background of 8%, statistically distinguishable from the F_1 value of 12.4% ± 1.8% red colonies ($P < 0.0001$, one-sample t-test).

DISCUSSION

We have established methods to produce knockout rats and have identified knockouts for Brcal and *Brca2*. Our technology combines protocols for efficient rat germline mutagenesis by ENU and a yeast-based method to economically (~$18,000 for a 90% chance of success) and rapidly screen preweanling F_1 rat pups from mutagenized fathers for functional mutations in selected genes using yeast truncation assays. The first identified rat gene to be knocked out, *Brca2*^{ochre4254}, was bred to homozygosity and has a phenotype that includes general growth inhibition and gonadal atrophy in both sexes. Interestingly, *Brca2* homozygous knockout mice with similar mutations in exon 11 have shown either embryonic lethality or embryonic survival with premature death[12–14]. We have not yet begun phenotypic evaluation of the Brcal knockout rat line.

Our ENU assay for the rat provides a phenotype-driven, ENU-induced mutation screening for a second murine species. The outbred SD rat tolerated the highest single and split dose of ENU. This and its ability to produce large litters led us to choose it for our genotype-based mutation screening. The inbred F344 strain tolerated higher doses than the very ENU-sensitive WF strain. It will be important in the future to evaluate additional inbred lines for their reproductive tolerance of ENU, as inbred rats provide a more homogenous genome than the more complex outbred rat strains, especially if evaluation of preexisting germline mutations is required. However, with either an inbred or outbred strain, it is important to backcross the knockout founder to either the isologous strain or another of a desired genetic background to eliminate other ENU-induced germline mutations. Switching genetic backgrounds may be more efficient in that it allows the use of speed congenic protocols. Furthermore, to eliminate the possible confounding effects of very closely linked mutations, one can screen for additional alleles of each knockout using this yeast-based technology and evaluate them phenotypically

Our yeast-based truncation screening assays have advantages and disadvantages that suggest which one should be used to target specific genes. The gDNA assay is most efficient if the selected gene has at least one exon larger than ~400–500 bp. In contrast, the cDNA assay is independent of exon size and can easily incorporate up to ~2,500 bp per vector. However, the background rate of red colony formation is over an order of magnitude lower in the gDNA assay, making it easier to identify mutant rats through red colony formation on the yeast plates. These truncation assays allow screening only for mutations that compromise protein translation, such as nonsense mutations and out-of-frame frameshift deletions or insertions. The Brcal knockout rat was identified using a cDNA yeast truncation assay in the 3′ region of the Brcal gene that consists of a series of very small exons. None of the

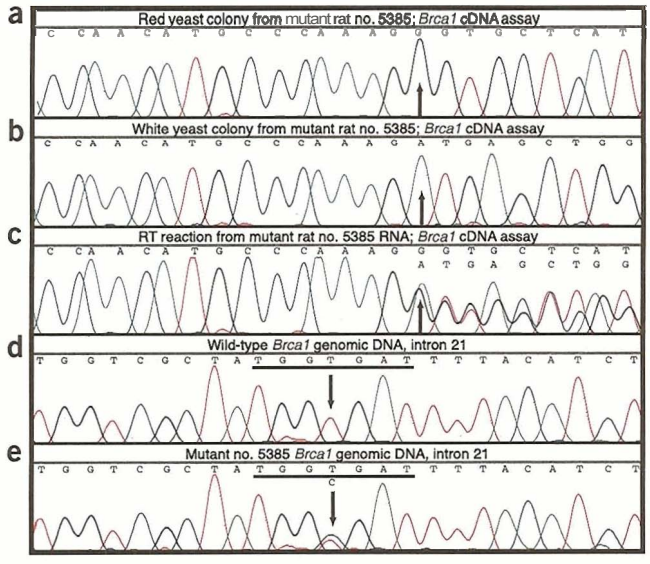

Figure 4 Screening for a *Brca1* knockout rat. Yeast cells were transformed with linearized gap vector and a PCR product enriched for *Brca1* fragment 3 (nucleotides 3974–5548). A plate with 44.3% red colonies (as compared to an average 15.8% red colony background from all other plates, $n = 89$) identified a potential knockout rat, no. 5385. (**a**) Sequence of haploid DNA from a yeast red colony (representative of eight colonies tested) in which exon 22 (74 bp) is deleted. (**b**) The sequence of haploid DNA from a wild-type white colony (representative of two colonies tested). The arrow in panel a indicates the first nucleotide (5359) of exon 23, whereas the arrow in panel b indicates the first nucleotide (5285) of exon 22. (**c**) This difference is highlighted by sequencing a mixture of cDNA from both rat alleles (+/–) from a reverse transcription reaction of total tail RNA (representative of two independent tests). In panels a, b and c, the sequence before the arrow is the 3′ end of exon 21. (**d**) Results of sequencing gDNA from a wild-type SD rat over a region of intron 21 that contains the splicing branch site (underlined). (**e**) The same sequence from the heterozygous *Brca1* mutant founder rat no. 5385, which includes a T→C mutation (indicated by the arrow) within the splicing branch site. Sequences in d and e span nucleotides 36–12 upstream of exon 22, with the mutation at nucleotide 24 upstream of exon 22. The mutant sequence is shown in its translated form in Supplementary Figure 2 online.

exons covered would have been good targets for the gDNA truncation assay because of their small size. In addition, this intronic mutation would not have been found using other screening methods, such as sequencing, heteroduplex analysis or denaturing high-performance liquid chromatography, because these assays are used to screen only the exons from gDNA.

The major drawbacks of the cDNA assay are that the gene-specific RNA may not be produced in an easily collectible tissue and mutant RNA may be lost to a great extent by NMD. In these studies, we demonstrate the ability of a cDNA yeast-based screening assay to detect the A mutant allele despite a high level of NMD in this model, and thus show the general ability of a yeast-based screening assay to detect mutants in spite of extensive NMD. NMD can be minimized by pretreating collected cells, such as white blood cells, with a protein synthesis inhibitor before RNA collection. This approach has been successful for the yeast gap-repair p53 assay[15,16] and may be extrapolated to in vivo studies by the administration of a protein synthesis inhibitor to rat pups before tissue collection. We have had preliminary success in inhibiting NMD using the protein synthesis inhibitor emetine. The problem of a gene-specific RNA not being produced in tail tissue may be reduced by extending the range of biopsy tissues collected from viable rats (for example, white blood cells, liver and skin). In the future, sperm from F_1 male rats of mutagenized fathers could be cryopreserved[17], and a wide variety of organ-specific RNAs could also be collected and stored, along with DNA from spleens or other tissue from the same male rats. DNAs or RNAs from a large number of rats could thus be screened and the appropriate frozen sperm used to recover mutant rats. Sperm cryopreservation has been established for many mouse strains and crosses[k8] and has allowed the recovery of a mutant mouse[kg].

In summary, the technologies presented here provide the means for producing gene-selected knockout lines for the rat. The generation of unique rat models should extend our knowledge of the genetics underlying human diseases and aid in the development of novel drugs to prevent and treat these diseases.

METHODS

Rat ENU mutagenesis protocol. The University of Wisconsin-Madison Animal Care and Use Committee has approved all experimental animal procedures described in these studies. We administered a single or split dose of ENU by intraperitoneal injection to male rats from Harlan at 9 weeks of age; for a split dose, at 9 and 10 weeks of age. One gram of ENU (Sigma) was dissolved in 10 ml of 95% (vol/vol) ethanol and then diluted with 90 ml of phosphate citrate buffer (0.2 M Na_2HPO_4, 0.1 M citric acid, pH 5.0) before injection. We paired mutagenized males with females of the same strain for consecutive 2- to 3-week periods, beginning 3–5 weeks after the first ENU treatment. We observed female rats for vaginal plugs, gross pregnancy, date of birth and size of litters. For our *Brca1* and *Brca2* mutation screening experiments, we used SD male rats given a split dose of ENU, 2 × 60 mg/kg body weight.

We collected tail dips from the F_1 pups at 1 week of age for macromolecule isolation. We also visually checked all F_1 pups for gross abnormalities in physical development at least twice before weaning at 21–28 d of age. A subset of the F_1 phenotypic mutant rats identified was bred to same-strain rats to determine inheritance of the phenotypic mutation. Several of the rat lines with heritable mutant phenotypes are currently being maintained and backcrossed to eliminate residual ENU-induced genetic changes not associated with the phenotypic mutations.

All breedings to produce ACI and (SD × ACI) F_1 pups were performed at our facility. At 3–7 d of age, pups were killed and ventral skin was collected for the A yeast assay.

Vector construction. The gap vector pLSRP53 containing the p53 cDNA[15,20] was digested with *Hin*dIII and *Eag*I to remove the entire p53 coding sequence. A 44-bp linker that contains sequence encoding the first 11 amino acids of rat p53 was inserted at the *Hin*dIII and *Eag*I sites to produce vector pLSK846 with the *Eag*I site converted to a unique NotI site. The full length *ADE2* gene was amplified by PCR from yeast strain yIG397 (ref. 15) DNA and integrated into the pLSK846 plasmid at the NotI site to generate vector pLSK870. A unique NotI site was retained at the 5′ end of the *ADE2* gene. This NotI site was used to drop in *Brca1*, *Brca2* or *A* sequence cassettes. Each *Brca1*, *Brca2* or *A* cassette contained two fused ~100 bp fragments, corresponding to the 5′ and 3′ ends of a ~1.6 kb *Brca1* fragment, a ~1.7 kb *Brca2* fragment or the ~500 bp A ORF, joined by a unique *Sma*I site. The half-site sequences of the *Brca1*, *Brca2* or *A* cassettes were designed to be in frame with the p53 leader and *ADE2* sequences (Fig. 2). Vectors were linearized before yeast transformation by digestion with SmaI (20 U/μl) and then purified using a QIAquick PCR purification kit (Qiagen, Inc.).

DNA/RNA extraction. To isolate DNA, small sections of tails were digested overnight at 55 °C in 500 μl of genomic lysis buffer consisting of 20 mM Tris-HCl, pH 8.0, 150 mM NaCl, 100 mM EDTA and 1% (wt/vol) SDS. Two hundred μl of Protein Precipitation Solution (Gentra Systems) was added to the lysate solution. DNA in the clear supernatant was precipitated with isopropanol, washed and resuspended in water. Total RNA was isolated from tail or skin sections that were placed in RNAzol B solution (Tel-Test) and homogenized (Polytron PT10-35, Kinematica). The samples were then extracted with

chloroform, precipitated with isopropanol and washed with ethanol. Pellets were resuspended in 30 µl RNA suspension solution (Ambion) for Brcal and *Brca2*, and in 60 µl for A.

Reverse transcription and PCR All primers used are listed in Supplementary Table 2 online. cDNA was synthesized for Brcal or *Brca2* from 1–2.5 µg rat tail total RNA at 42 °C for 2 h with 200 U of Superscript II (Invitrogen). A cDNA was synthesized from 1–5 µg of skin total RNA in a 1 h reaction. The 20 µl reaction consisted of 1× reverse transcription buffer (Invitrogen), 0.5× RNA secure reagent (Ambion), 10 mM DTT, 1.25 mM dNTP mix and 0.33 µg *Brca1*-, *Brca2*-, or A-specific primers. PCR was performed on 1.0 µl of the cDNA product or ~0.1 µg of gDNA with 1 U of Herculase (Stratagene) in 20 µl reactions containing 1x Herculase Buffer, 0.2 mM dNTP mix and 0.05 µg primers for Brcal and *Brca2*. Reaction conditions for Brcal and *Brca2* fragments were 95 °C for 2 min, followed by 35 cycles consisting of 1 min at 92 °C, 45 s at 60 °C, and 4 min at 72 °C, followed by 7 min at 72 °C. For the A gene PCR, 0.5 U of Failsafe enzyme (Epicentre Technologies) was used with Failsafe buffer J (which contains dNTPs) and 0.1 µg primers. The cycling conditions for A were similar to above except that the annealing temperature was 55 °C and the 72 °C extension step was only 1 min. PCR quality and product quantity were estimated by electrophoresis in a 1.2% (wt/vol) agarose gel.

Yeast transformation and sequencing. yIG397 (ref. 15) yeast was cultured overnight at 30 °C in YPD medium supplemented with adenine (200 µg/ml) to an OD_{600} of 0.9. The cells were washed and resuspended in a volume of LiOAc/TE solution (0.1 M lithium acetate, 10 mM Tris-HCl, pH 8.0, 1 mM EDTA) equivalent to the volume of the cell pellet. For each transformation, 30 µl of yeast suspension was mixed with 10 ng of linearized gap vector, 25 µg of salmon sperm carrier DNA, 150 µl of LiOAc/TE/PEG solution (0.1 M lithium acetate, 10 mM Tris-HCl, pH 8.0, 1 mM EDTA, 40% (wt/vol) PEG) and 2–5 µl unpurified Brcal, *Brca2*, or A PCR product (total volume ~185 µl). The mixture was incubated for 30 min at 30 °C, then heat-shocked for 15 min at 42 °C. Transformants were then plated on synthetic minimal medium lacking leucine and supplemented with low adenine (5 µg/ml) and incubated for 3 d at 30 °C. An automated colony counter (ProtoCOL, Microbiology International) was used to determine the number of red and white colonies on each plate for the cDNA assays, and the percentage of red colonies per sample was recorded. The background rate of red colonies was determined by averaging the percentage of red colonies from all plates not containing a knockout. gDNA assay yeast plates were generally inspected only visually. The signal-to-noise ratio for the gDNA assay was large (>50:1), whereas that for the cDNA assay was smaller (~3:1). Thus, a criterion for the cDNA assays was set to follow up on samples for which the red colony percentage was at least 2 s.d. above the mean. This conservative criterion was designed to avoid false negatives and on average resulted in two false positives per gene assay for 90 rats screened. Most false positives were eliminated upon repeating the yeast assay using the original RNA sample.

For sequencing, red and white colonies were picked directly into PCR mix, amplified and purified to remove primers and nucleotides. Four microliters of each reaction was then used in a 20 µl cycle-sequencing reaction using BigDye (Applied Biosystems Inc.) chemistry.

Note: *Supplementary information* is available on the Nature *Biotechnology website.*

ACKNOWLEDGMENTS
We thank Amy Moser for discussions and suggestions during the course of this work; R. Iggo, M. Tada, and T. Moriuchi for providing the pLSRP53 plasmid and the yIG397 yeast strain used in this paper; Henry Pitot for analysis of the histology sections; and Dinelli M. Monson and Millicent A. Shultz for technical assistance. This work has been supported by grants from the US National Institutes of Health (CA28954 and CA77494).

COMPETING INTERESTS STATEMENT
The authors declare that they have no competing financial interests.

Received 24 September 2002; accepted 13 March 2003
Published online 18 May 2003; doi:10.1038/nbt830

1. Jacob, H.J. & Kwitek, A.E. Rat genetics: attaching physiology and pharmacology to the genome. Nat. Rev. Genet. 3, 33-42 (2002).
2. Justice, M.J., Noveroske, J.K., Weber, J.S., Zheng, B. & Bradley, A. Mouse ENU mutagenesis. Hum. Mol. Genet. 8, 1955–1963 (1999).
3. Noveroske, J.K., Weber, J.S. & Justice, M.J. The mutagenic action of *N*-ethyl-*N*-nitrosourea in the mouse. Mamm. Genome 11,478–483 (2000).
4. Russell, W.L. et al. Specific-locus test shows ethylnitrosourea to be the most potent mutagen in the mouse. *Proc.* Natl. Acad. Sci. USA 76, 5918–5922 (1979).
5. Beier, D.R. Sequence-based analysis of mutagenized mice. Mamm. Genome 11, 594–597 (2000).
6. Justice, M.J. et al. Effects of ENU dosage on mouse strains. Mamm. Genome 11, 484–488 (2000).
7. Ishioka, C. et al. Screening patients for heterozygous p53 mutations using a functional assay in yeast. Nat. Genet. 5, 124–129 (1993).
8. Kataoka, A. et al. Development of a yeast stop codon assay readily and generally applicable to human genes. Am. J. Pathol. 159, 1239–1245 (2001).
9. Culbertson, M.R. RNA surveillance. Unforeseen consequences for gene expression, inherited genetic disorders and cancer. *Trends* Genet. 15, 74–80 (1999).
10. Frischmeyer, P.A. & Dietz, H.C. Nonsense-mediated mRNA decay in health and disease. Hum. Mol. Genet. 8, 1893–1900 (1999).
11. Kuramoto, T., Nomoto, T., Sugimura, T. & Ushijima, T. Cloning of the rat agouti gene and identification of the rat nonagouti mutation. Mamm. Genome 12, 469–471 (2001).
12. Suzuki, A. et al. *Brca2* is required for embryonic cellular proliferation in the mouse. Genes *Dev.* 11,1242–1252 (1997).
13. Connor, F. et al. Tumorigenesis and a DNA repair defect in mice with a truncating *Brca2* mutation. Nat. Genet. 17, 423–430 (1997).
14. Freidman, L.S. et al. Thymic lymphomas in mice with a truncating mutation in *Brca2*. Cancer Res. 58, 1338 1343 (1998).
15. Flaman, J.-M. et al. A simple p53 functional assay for screening cell lines, blood, and tumors. *Proc.* Natl. Acad. Sci. USA 92,3963–3967 (1995).
16. Andreutti-Zaugg, C., Scott, R.J. & Iggo, R. Inhibition of nonsense-mediated messenger RNA decay in clinical samples facilitates detection of human MSH2 mutations with an in *vivo* fusion protein assay and conventional techniques. Cancer *Res.* 57. 3288–3293 (1997).
17. Nakatsukasa, E. et al. Generation of live rat offspring by intrauterine insemination with epididymal spermatozoa cryopreserved at −196 °C. *Reproduction* 122, 463–467 (2001).
18. Nakagata, N. Cryopreservation of mouse spermatozoa. Mamm. Genome 11,572–576 (20001.
19. Coghill, E.L. et al. A gene-driven approach to the identification of ENU mutants in the mouse. Nat. Genet. 30, 255–256 (2002).
20. Yamamoto, K. et al. A functional and quantitative mutational analysis of p53 mutations in yeast indicates strand biases and different roles of mutations in DMBA- and BBN-induced tumors in rats. Int. J. *Cancer* 83, 700–705 (1999).

Oncogene (2007) 26, 1626–1635

www.nature.com/onc

ORIGINAL ARTICLE

Characterizing a rat *Brca2* knockout model

MS Cotroneo[1,7], JD Haag[1,7], Y Zan[1], CC Lopez[1], P Thuwajit[1], GV Petukhova[2], RD Camerini-Otero[2], A Gendron-Fitzpatrick[3], AE Griep[4], CJ Murphy[5], RR Dubielzig[6] and MN Gould[1]

[1]*McArdle Laboratory for Cancer Research, University of Wisconsin-Madison, Madison, WI, USA;* [2]*Genetics and Biochemistry Branch, National institute of Diabetes and Digestive and Kidney Diseases, National Institutes of Health, Bethesda, MD, USA;* [3]*Comparative Pathology Laboratory, Research Animals Resource Center, University of Wisconsin-Madison, Madison, WI, USA;* [4]*Department of Anatomy, University of Wisconsin Medical School, Madison, WI, USA;* [5]*Department of Surgical Sciences, School of Veterinary Medicine, University of Wisconsin-Madison, Madison, WI, USA and* [6]*Department of Pathobiological Sciences, School of Veterinary Medicine, University of Wisconsin-Madison, Madison, WI, USA*

Evidence exists that *BRCA2* carriers may have an elevated risk of breast, ovarian, colon, prostate, and pancreatic cancer. In general, carriers are defined as individuals with protein truncating mutations within the *BRCA2* gene. Many *Brca2* knockout lines have been produced and characterized in the mouse. We previously produced a rat *Brca2* knockout strain in which there is a nonsense mutation in exon 11 between BRC repeats 2 and 3, and a truncated protein is produced. Interestingly, while such a mutation in homozygous mice would lead to limited survival of approximately 3 months, the *Brca2*$^{-/-}$ rats are 100% viable and the vast majority live to over 1 year of age. *Brca2*$^{-/-}$ rats show a phenotype of growth inhibition and sterility in both sexes. Aspermatogenesis in the *Brca2*$^{-/-}$ rats is due to a failure of homologous chromosome synapsis. Long-term phenotypes include underdeveloped mammary glands, cataract formation and lifespan shortening due to the development of tumors and cancers in multiple organs. The establishment of the rat *Brca2* knockout model provides a means to study the role of *Brca2* in increasing cancer susceptibility and inducing a novel ocular phenotype not previously associated with this gene.
Oncogene (2007) **26,** 1626–1635. doi:10.1038/sj.onc.1209960; published online 11 September 2006

Keywords: Brca2; knockout; rat; carcinogenesis; tumors

Introduction

Mutation of the highly penetrant tumor suppressor gene *BRCA2* has been associated with a wide range of phenotypes, characterized by an increased susceptibility to breast, ovarian and other cancers. In addition, mutant *BRCA2* is associated with Fanconi's anemia. Cell culture studies indicate that BRCA2 has several functions, including repair of double-strand breaks (DSBs) in DNA through homologous recombination, as well as regulation of transcription and the cell cycle (reviewed by Yoshida and Miki, 2004). It is hypothesized that tumor suppression by BRCA2 is related to its ability to repair DSBs through interaction with the RAD51 recombination enzyme (Shivji and Venkitaraman, 2004). This interaction is mediated by conserved amino-acid motifs (BRC repeats) within exon 11 of BRCA2 (Bork *et al*., 1996; Bignell *et al*., 1997).

While there are *in vivo* mouse models of human disease to study the inactivation of the *Brca2* gene by truncating mutations, the models are somewhat limited by low viability of *Brca2* mutant mice. Homozygous mice with severe truncations of the Brca2 protein before exon 11 or resulting in the deletion of this exon are embryonic lethal (reviewed by Moynahan, 2002). Homozygous *Brca2* knockout mice with some of the BRC repeats in exon 11 left intact are infertile, have a limited life span and develop thymic lymphoma (Connor *et al*., 1997; Friedman *et al*., 1998). In contrast, truncation of a small region of the carboxyl end of Brca2 results in fertile animals with no gross abnormalities that are predisposed to cancer (McAllister *et al*., 2002), although there is $\sim$30% reduced viability than expected for homozygous mice. Other mouse models with improved viability are available, but often require multiple genetic manipulations to improve survivability (reviewed by Moynahan, 2002). Therefore, we sought to produce an additional genetic tool by using a rat model to study *Brca2* function.

Our group has developed a technology that for the first time can produce knockout rats using ENU mutagenesis with a yeast-based screening procedure to identify functional mutations of specific genes (Zan *et al*., 2003). The first knockout rat produced was for the *Brca2* gene. We previously reported that the ENU-induced nonsense mutation generated a stop codon located 5′ of the well conserved BRC repeats in exon 11. The major short-term phenotypes previously reported for the homozygous *Brca2* knockout rat were stunted growth and sterility in both males and females. Here, we

Correspondence: Dr MN Gould, McArdle Laboratory for Cancer Research, University of Wisconsin-Madison, 1400 University Avenue, Madison, WI 53706, USA.
E-mail: gould@oncology.wisc.edu
[7]These authors contributed equally to this work.
Received 16 May 2006; revised 18 July 2006; accepted 21 July 2006; published online 11 September 2006

report the long-term phenotypes observed in rat *Brca2* knockouts.

Results

Truncated protein

Western blotting with anti-Brca2 indicated the presence of full length Brca2 (~372 kDa) in testes extracts from $Brca2^{+/+}$ and $Brca2^{+/-}$ rats (Figure 1a). In $Brca2^{-/-}$ samples, no full length Brca2 band was observed, even with extended exposure of the membrane to the film (not shown). Based on the position of the *Brca2* mutation (Zan *et al*., 2003), the predicted size of truncated Brca2 protein is ~150 kDa. A truncated Brca2 product of the expected size was detected in $Brca2^{+/-}$ and $Brca2^{-/-}$ samples after extended exposure of the lower portion of the blot (Figure 1b), but was not observed in the $Brca2^{+/+}$ testis.

Growth inhibition phenotype

As was previously reported, $Brca2^{-/-}$rats exhibit growth inhibition before weaning and up to 14 weeks of age. This reduction in body weight continues for both $Brca2^{-/-}$ male and female rats throughout their life span, while $Brca2^{+/-}$ rats maintain body weights very similar to the $Brca2^{+/+}$ rats (data not shown). At approximately 1 year of age, the reduction in body weight for $Brca2^{-/-}$rats compared to $Brca2^{+/+}$ littermate controls was 33 and 21% for male and females, respectively.

Underdeveloped mammary gland phenotype

$Brca2^{-/-}$ rats are sterile due to ovarian and testicular atrophy (Zan *et al*., 2003). In addition, the mammary glands of $Brca2^{-/-}$ female rats are underdeveloped. Analysis of mammary gland morphology in adult *Brca2* female rats ($n = 4$–5 rats/genotype) revealed that the $Brca2^{-/-}$ rat mammary gland was smaller and less developed than that from wild-type and heterozygous rats (Figure 2a). The $Brca2^{-/-}$ mammary glands did show estrogen-responsiveness, as the size of mammary glands from $Brca2^{-/-}$ rats following ovariectomy and estrogen replacement was similar to that of $Brca2^{+/+}$ and $Brca2^{+/-}$ rats given this treatment (Figure 2b).

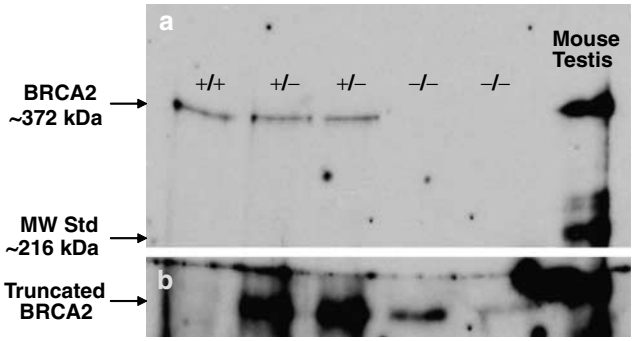

Figure 1 $Brca2^{-/-}$rats lack full length Brca2 protein (**a**) and have a truncated Brca2 product (**b**). Western blotting analysis of testes extracts with anti-Brca2 indicates full length Brca2 protein (~372 kDa) in $Brca2^{+/-}$, $Brca2^{+/+}$ and mouse (control) testis samples after a 1 min exposure of the membrane to film (**a**). (**b**) shows the bottom portion of the blot after extended exposure time. A truncated Brca2 protein of the expected size as indicated by the arrow is present in the $Brca2^{-/-}$ and $Brca2^{+/-}$ samples but absent in the $Brca2^{+/+}$ testis sample. MW Std; molecular weight standard.

Aspermatogenesis

Meiosis in $Brca2^{-/-}$ rats proceeds normally through leptotene and early zygotene (Figure 3a) with 40 centromeres clearly identified by CREST antisera (Brenner *et al*., 1981). The correct number of centromeres and chromosome cores indicates that sister chromatid cohesion is not affected in the absence of Brca2. Immunostaining for the Scp3/Cor1 protein of axial/lateral elements (Dobson *et al*., 1994) revealed that homologous chromosomes are not assembled into the synaptonemal complex (Figure 3b). Even though the chromosomes in arrested $Brca2^{-/-}$ spermatocytes look rather compact, only limited synapsis could be seen in a fraction of cells. Synapsed regions could be detected by staining for the Scp1/Syn1 protein, a component of the central element of the synaptonemal complex (Dobson *et al*., 1994). The most advanced $Brca2^{-/-}$ spermatocytes show short stretches of synapsed regions, presumably between nonhomologous chromosomes. Cells with rather extensive synapsis are rare.

Spo11-mediated DSBs initiate meiotic homologous recombination and the repair of these breaks is required for chromosome synapsis in most organisms including mammals (Roeder, 1997; Zickler and Kleckner, 1999; Keeney, 2001; Villeneuve and Hillers, 2001). The appearance of the breaks in leptotene is accompanied by the phosphorylation of histone H2ax over megabase-size chromatin regions (Mahadevaiah *et al*., 2001). In $Brca2^{+/+}$ rat spermatocytes this stage can be easily recognized by anti-γH2ax (phosphorylated H2ax) antibodies that produce a cloud-like staining pattern all over the chromatin (Figure 4a). By pachytene (Figure 4b), γH2ax staining remains only in the sex body region (Eijpe *et al*., 2000; Mahadevaiah *et al*., 2001). $Brca2^{-/-}$ spermatocytes show extensive γH2ax staining that persists to the most advanced stages with the maximum extent of synapsis (Figure 4c and d). These data indicate that DSBs are generated in the $Brca2^{-/-}$ knockout spermatocytes but are not repaired.

Cancer/tumor incidence in Brca2$^{-/-}$ *rats*

N2 × N2 male and female rats were followed for up to 24 months to determine if tumors and/or other pathologies would develop in the $Brca2^{-/-}$animals, compared with $Brca2^{+/-}$ and $^{+/+}$ littermate controls. Some animals were necropsied before this time point, if signs of morbidity were observed. This was true for many $Brca2^{-/-}$ rats, as they developed a variety of tumors and/or appeared moribund around 1 year of age. The average life span (Figure 5a) for $Brca2^{-/-}$ males ($n = 16$) was 14 months of age compared to 21 months for $Brca2^{+/-}$ and $^{+/+}$ rats ($n = 52$, $n = 19$, respectively). Similarly, $Brca2^{-/-}$ females ($n = 33$) had an average life

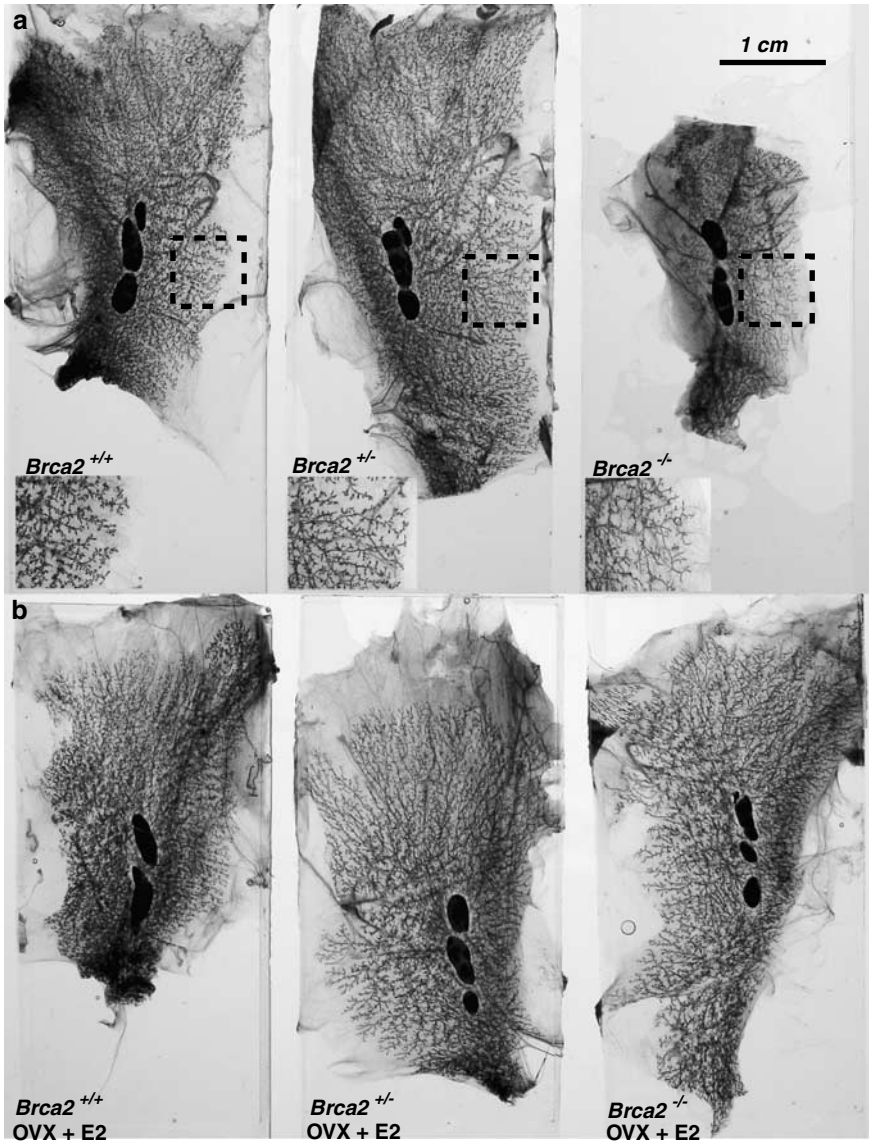

Figure 2 Underdeveloped mammary glands from *Brca2*$^{-/-}$ rats (**a**) are responsive to short term estrogen replacement following ovariectomy (OVX + E2) (**b**). Aluminum carmine stained whole mounts of the fourth (abdominal) mammary gland from 12-week old rats. (**a**) Mammary glands from untreated *Brca2*$^{+/+}$, *Brca2*$^{+/-}$ and *Brca2*$^{-/-}$ rats with inset photos magnified to show detail of terminal edge of the mammary gland adjacent to the lymph node (bar = 1 cm). (**b**) Mammary glands from similar rats ovariectomized at 6 weeks of age and given 6 weeks of estrogen replacement with Silastic tubing implants containing β-estradiol.

span of 15 months of age versus 20–21 months for *Brca2*$^{+/-}$ and $^{+/+}$ rats ($n = 55$, $n = 28$, respectively) (Figure 5b).

The majority of rats on this long-term phenotyping study were necropsied and examined for disease. Cancer/tumor incidence was significantly increased in both male and female *Brca2*$^{-/-}$ rats, compared with *Brca2*$^{+/+}$ controls or heterozygous rats ($P < 0.0001$, Fisher's exact test). In male *Brca2*$^{-/-}$ rats, cancer/tumors were identified in 73% (11/15) of the rats examined, in contrast to *Brca2*$^{+/-}$ and $^{+/+}$ male rats, in which only 5% (2/40) and 0% (0/14) respectively, developed some type of abnormality. A similar trend of significantly increased cancer/tumor incidence of 67% (18/27) was seen in *Brca2*$^{-/-}$ female rats. *Brca2*$^{+/-}$ and *Brca2*$^{+/+}$ females had a cancer incidence of 12% (6/52) and 15% (4/27), respectively, due exclusively to cancers/tumors of the mammary gland (Figure 5d). As the number of benign mammary lesions in these rats was high, the analysis here includes only mammary carcinomas. Surprisingly, the frequency of mammary carcinoma development between females of the three *Brca2* genotypes was similar despite the observation that mammary glands of the *Brca2*$^{-/-}$ rats are underdeveloped and ovarian function appears to be limited in these rats.

The most prevalent tumor types observed in *Brca2*$^{-/-}$ rats were sarcomas located in stomach, muscle and bone (Figures 5c, d and 6a). Several of the osteosarcomas appeared to have developed in the rear limbs or

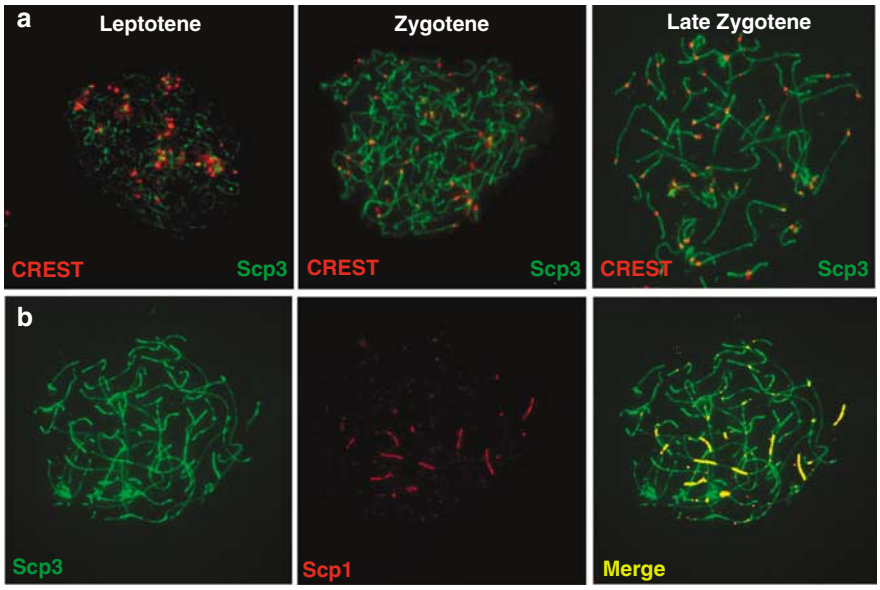

Figure 3 (**a**) Meiosis in *Brca2*$^{-/-}$ spermatocytes does not progress beyond late zygotene. Chromosomal spreads were prepared from spermatocytes of adult *Brca2*$^{-/-}$ rats and immunostained with Scp3 and CREST antisera. Stages of the first meiotic prophase are indicated. (**b**) Immunostaining for Scp3 and Scp1, demonstrating the limited degree of synapsis of homologous chromosomes that occurs in *Brca2*$^{-/-}$ spermatocytes.

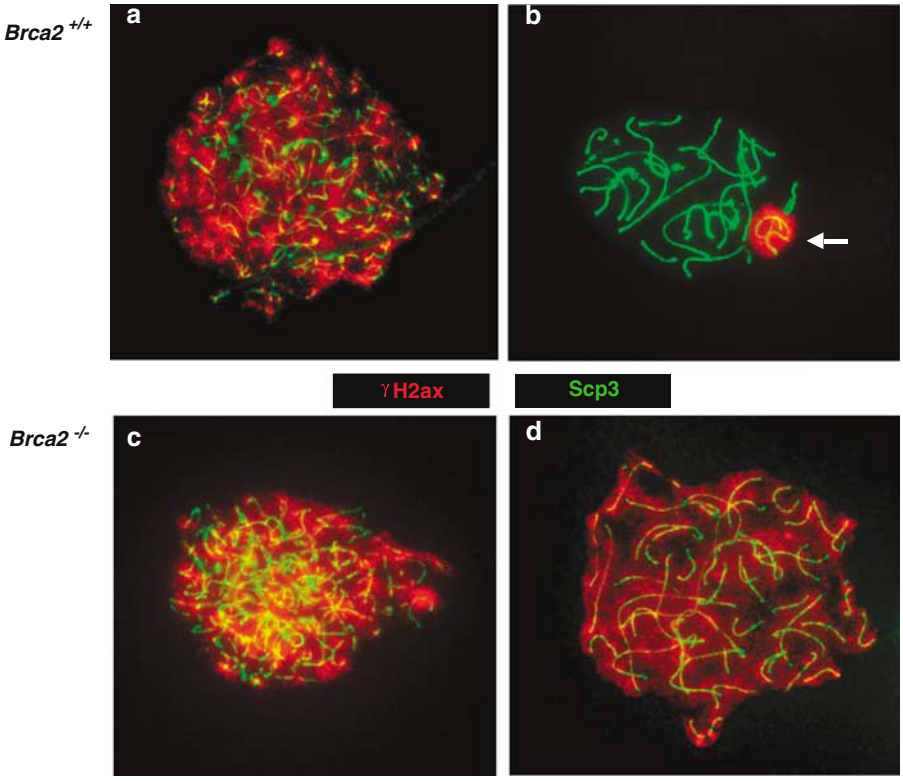

Figure 4 Meiotic DSBs are formed but not repaired in *Brca2*$^{-/-}$ spermatocytes. Chromosomal spreads were prepared from *Brca2*$^{+/+}$ or *Brca2*$^{-/-}$ spermatocytes of adult rats and immunostained with γH2ax and Scp3 antisera, as indicated. Leptotene spermatocytes are shown in (**a**) and (**c**), pachytene in (**b**), and late zygotene in (**d**). Arrow indicates a sex body.

sternum, and in four cases, the sarcomas metastasized to lung tissue. In addition, approximately 20% of female *Brca2*$^{-/-}$ rats developed ovarian tumors, including granulosa cell tumors and thecomas (Figure 6b and c).

Cataract formation

At approximately 6–9 months of age, cataracts were visible in several of the *Brca2*$^{-/-}$ rats, while none were seen in heterozygous or wild-type controls. Clinical

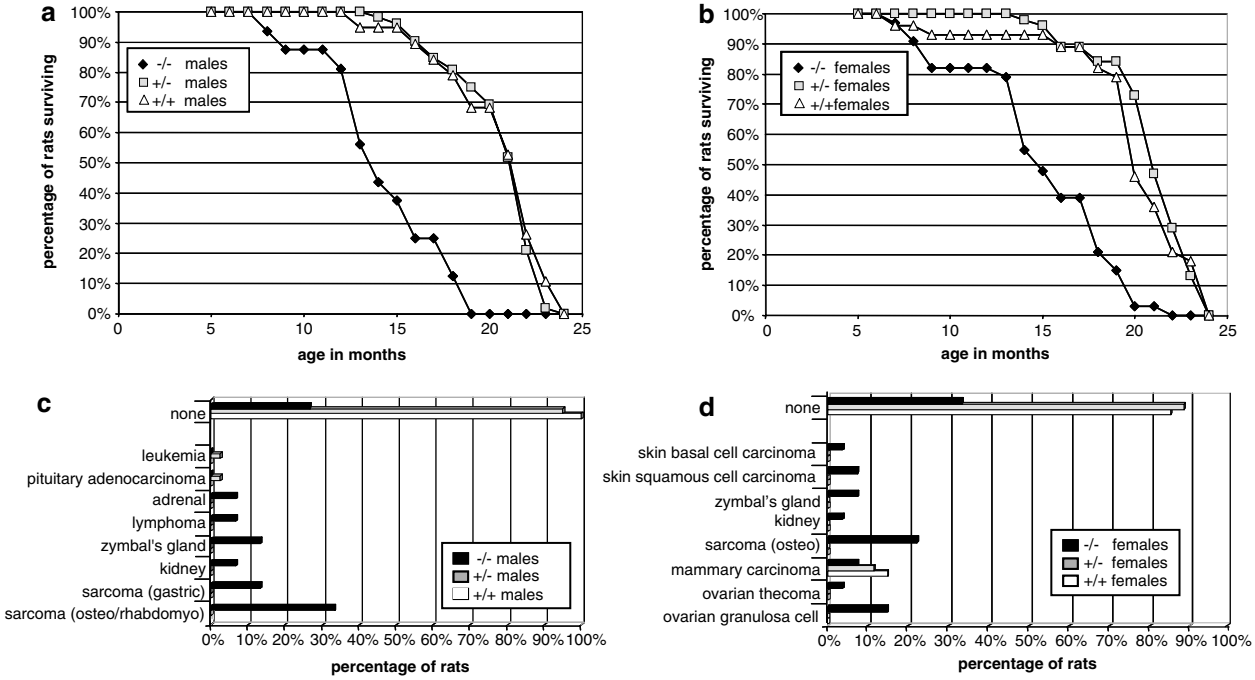

Figure 5 Reduced survival is observed in male (**a**) and female (**b**) *Brca2*$^{-/-}$ rats, compared with heterozygous and wild-type rats. Increased incidence of various tumors/cancers in male (**c**) and female (**d**) *Brca2*$^{-/-}$ knockout rats is also observed.

assessment of ocular pathology was carried out on *Brca2*$^{-/-}$ ($n=78$ eyes, 39 rats), *Brca2*$^{+/-}$ ($n=12$ eyes, 6 rats), and *Brca2*$^{+/+}$ ($n=12$ eyes, 6 rats) rats of 11–14 months of age by slit lamp examination. Greater than 90% of *Brca2*$^{-/-}$ rats showed various anterior segment disorders, whereas *Brca2*$^{+/-}$ or *Brca2*$^{+/+}$ rats did not. Cataracts, including cortical and anterior, were observed in >90% of the *Brca2*$^{-/-}$ rats. Collapsed anterior chamber was observed in 23% of the *Brca2*$^{-/-}$ rats and synechiae were observed in 38% of the *Brca2*$^{-/-}$ rats (Figure 6d). Histopathologic assessment of eyes from *Brca2*$^{-/-}$ rats was consistent with findings of the slit lamp examination. Analysis of hematoxylin and eosin-stained sections showed various cataracts (cortical, anterior, equatorial and posterior) in 84% (11/13) of the *Brca2*$^{-/-}$ animals. A variety of other abnormalities including synechiae, lens mineralization, posterior lens capsule rupture and anterior segment dysgenesis also were frequently observed.

Discussion

Rat knockout models have the potential to not only complement mouse knockouts, but also identify novel phenotypes and gene functions in models of human disease. The first knockout rat produced was for the *Brca2* tumor suppressor gene. As previously reported, short-term phenotypic analysis of the *Brca2* knockout rats showed that heterozygous animals could be bred to yield viable homozygous offspring despite having a severe protein truncation in the beginning of exon 11 that removes all highly conserved BRC repeats (Zan *et al*., 2003).

This exon 11 mutation in the *Brca2* gene was predicted to produce a truncated Brca2 product of approximately 150 kDa (Zan *et al*., 2003). We did not detect full-length or truncated Brca2 product in the spleens, kidneys, mammary glands or ovaries of animals from all *Brca2* gentoypes (data not shown), presumably due to low expression levels. Therefore, we cannot speculate as to the potential for truncated Brca2 products with reduced or alternative functions in these or other tissues. We assessed for truncated Brca2 products in the testes, due high expression levels of Brca2 in this tissue. A weakly expressed band of the expected size was observed in the testes samples from *Brca2*$^{-/-}$ and *Brca2*$^{+/-}$ rats but not in the wild-type. No full-length Brca2 was found in *Brca2*$^{-/-}$ samples. Expression of the truncated product was higher in the *Brca2*$^{+/-}$ testes extracts compared with the *Brca2*$^{-/-}$ samples despite loading equal amounts of total protein. This finding may be due to the dilution of proteins from apoptotic spermatocytes in *Brca2*$^{-/-}$ extracts by those expressed in viable cells. This is consistent with our previous observation of the lack of mature sperm cells in *Brca2*$^{-/-}$ testes (Zan *et al*., 2003).

Analysis of the infertility in *Brca2*$^{-/-}$ male rats revealed that aspermatogenesis was caused by the failure of homologous chromosome assembly at the synaptonemal complex. Current models (Allers and Lichten, 2001; Villeneuve and Hillers, 2001) suggest that the major event in meiotic recombination is the Rad51/Dmc1-mediated homology search followed by the single end invasion (Hunter and Kleckner, 2001) of the intact

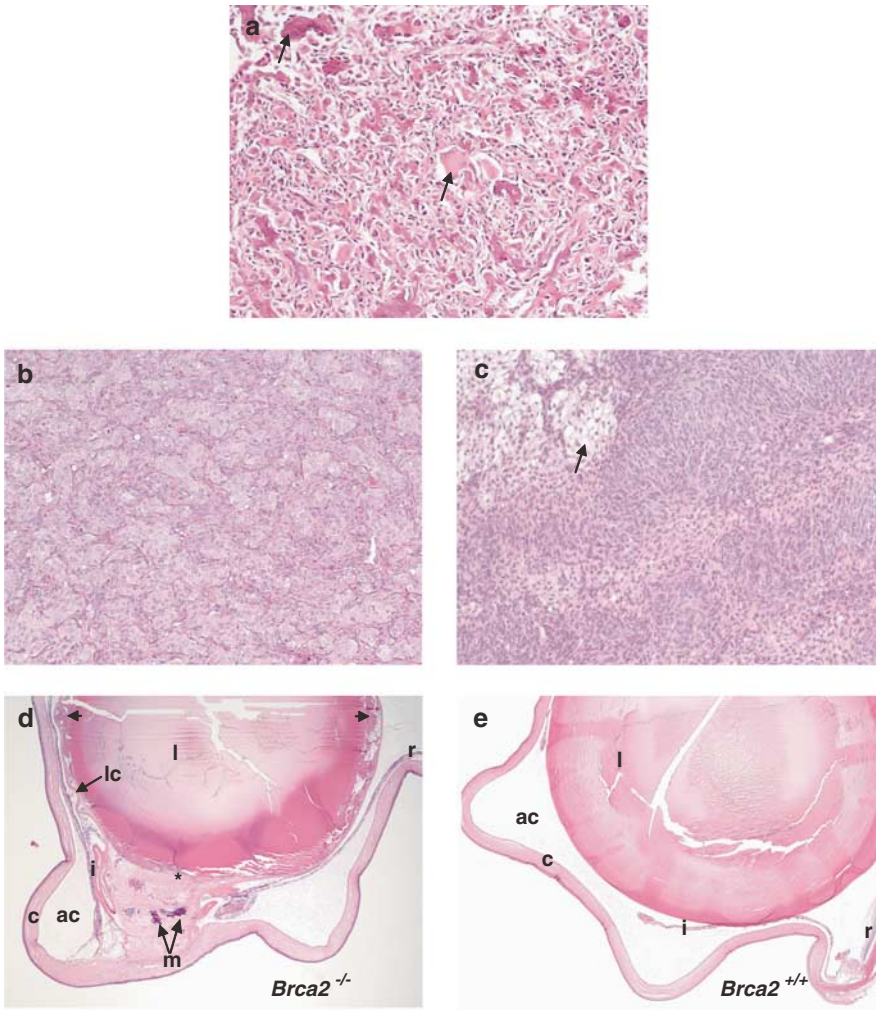

Figure 6 *Brca2*$^{-/-}$ rats have various tumors and pathologic changes, shown by hematoxylin and eosin staining of tissue sections. (**a**) Osteosarcoma composed of anaplastic cells and islands of tumor osteoid (arrows), ×20 magnification. (**b**) Ovarian granulosa cell tumor with follicular pattern, ×20 magnification. (**c**) Ovarian thecoma composed of densely packed fusiform cells with a focus of vaculated cells (arrow), ×20 magnification. (**d**) Eye from an adult rat with a hypermature cataract showing a ruptured lens capsule (lc), anterior subcapsular cataract (asterisk) with spindle cells and mineralization (m), a collapsed anterior chamber (ac), posterior synechiae (adhesion of iris to lens), and anterior segment dysgenesis (adhesion of lens to cornea). The cataractous lens cells extend circumferentially around the lens capsule to the posterior (arrowheads). ac, anterior chamber; c, cornea; i, iris; l, lens; lc, lens capsule; r, retina; m, mineralization, ×4 magnification. (**e**) Normal eye from *Brca2*$^{+/+}$ rat, ×4 magnification.

homologous chromosome. Rad51 and Dmc1 are believed to load onto the single-stranded ends of resected DSBs and can be observed as numerous foci on the chromosome cores. These foci disappear in pachytene, when the breaks are successfully repaired. Previous studies showed a decrease in Rad51 and Dmc1 foci in infertile *Brca2* knockout mice rescued from embryonic lethality by expression of human *BRCA2* gene (Sharan *et al*., 2004). However, rat *Brca2*$^{-/-}$ spermatocytes are completely devoid of either Rad51 or Dmc1 foci (data not shown). This finding is in agreement with a proposed role of BRCA2 in transporting Rad51 and Dmc1 to the sites of DNA damage (Davies *et al*., 2001; Siaud *et al*., 2004). Taken together, the observations of infertility, aspermatogenesis and meiotic prophase arrest suggest that the truncated Brca2 protein product identified in the rat testis is not functional. Interestingly, meiotic arrest during prophase is commonly observed in the testes of men with azoospermia (Schulze *et al*., 1999), and a potential association between the common *BRCA2* variant N372H has been identified in infertile men with azoospermia or oligospermia (Zhoucun *et al*., 2006). Therefore, this cell-specific function of BRCA2 identified in rodents may have implications in human infertility.

Although *Brca2*$^{-/-}$ rats are sterile and have lower body weights compared to *Brca2*$^{+/-}$ and *Brca2*$^{+/+}$ rats, all homozygous knockouts survive into adulthood. This finding is in contrast to homozygous *Brca2* knockout mice with similar mutations as these mice die early (reviewed by Moynahan, 2002). For long-term phenotypic analysis of *Brca2*$^{-/-}$ knockout rats, homozygous, heterozygous and wild-type littermates were monitored over their lifespan. The use of littermates minimizes the

possibility that the observed phenotypes were derived from 'passenger' mutations caused by ENU. We were able to both confirm *Brca2* related phenotypes observed in various mouse models and also extend these observations to a novel phenotype.

Male and female *Brca2*$^{-/-}$ rats were followed for their lifetime survivability and cancer incidence. In comparison to the *Brca2*$^{+/-}$ and *Brca2*$^{+/+}$rats, the *Brca2*$^{-/-}$ rats had a substantial reduction in lifespan for both sexes. At least part of this reduction in lifespan could be attributed to an increase in cancer development. The male *Brca2*$^{-/-}$ rats developed $\sim$15 times the number of tumors or cancers developing in the *Brca2*$^{+/-}$ and *Brca2*$^{+/+}$ rats. A similar trend also occurred in the female rats. The most prevalent tumor type in male *Brca2*$^{-/-}$ rats was sarcoma of the stomach, bone and muscle. Tumors arising most frequently in female *Brca2*$^{-/-}$ rats were osteosarcomas and ovarian tumors. *Brca2*$^{-/-}$ female rats (20%) developed ovarian tumors, including those of the thecal and granulosa cells.

Notably, osteosarcoma development in both male and female *Brca2*$^{-/-}$ rats occurred at a frequency of 20%, a site not common in the limited surviving mice having terminal deletions of exon 11 (Connor *et al*., 1997; Friedman *et al*., 1998). Homozygous deletion of exon 27 in mice resulted in the development of various epithelial carcinomas, lymphomas and sarcomas however, no osteosarcomas and only one ovarian tumor were reported (McAllister *et al*., 2002). In contrast, further studies showed significantly more osteosarcomas in homozygous mice lacking exon 27 than in their heterozygous or wild-type counterparts, an effect that was greatly enhanced when the mice were also heterozygous for mutant *p53* (McAllister *et al*., 2006). These authors point out that tumor spectrum in these models may be affected by the background strain genetics. It is also plausible to hypothesize that diminished DSB repair by lack of functional Brca2 may play a role in the development of osteosarcomas in *Brca2*$^{-/-}$ rats, as accumulation of DSBs can result in chromosomal translocations, a common finding in human sarcomas and hematologic malignancies (reviewed by Elliott and Jasin, 2002). Further analysis of tumors from *Brca2*$^{-/-}$ rats is needed to determine if their etiology is a direct result of loss of Brca2 function.

It is important to note that *Brca2*$^{-/-}$ females did not show increased propensity to develop mammary carcinomas, which may be due to the inhibition of mammary development resulting from lack of ovarian differentiation. Short-term estrogen replacement enhanced mammary development in ovariectomized *Brca2*$^{-/-}$ females. It is possible that if endocrinologic deficiencies could be restored long-term, increased mammary carcinoma development might be observed.

Finally, we observed ocular phenotypes that have not been previously reported to be associated with the inactivation of *Brca2* function. Most striking was the high incidence of cataracts in *Brca2*$^{-/-}$ rats, which may be a consequence of diminished repair of DSBs in the lens epithelium. Unrepaired DNA damage to the epithelial cells of the lens is thought to be related to cataract etiology (Worgul *et al*., 1991). Similarly, agents causing SSBs and DSBs, such as ionizing radiation received through therapeutic total body irradiation (Zierhut *et al*., 2000) or space travel (Cucinotta *et al*., 2001), are associated with increased susceptibility to cataract formation. Cells deficient in BRCA2, including those derived from mouse models with C-terminal truncating mutations show sensitivity to DSB formation, chromosomal damage, and cell death resulting from ionizing radiation (reviewed by Pellegrini and Venkitaraman, 2004).

Evidence from knockout mouse models of genes that interact with the BRCA2 pathway, such as ataxiatelangioectasia (*Atm*) and Fanconi Anemia (FA), also suggests that ocular abnormalities may arise from inefficient DSB repair. Mice heterozygous for the *Atm* gene are sensitive to radiation-induced cataracts (Worgul *et al*., 2002) and homozygous *Fancd2* knockout mice have micropthalmia (Houghtaling *et al*., 2003). In addition to abnormal ocular pathology, these models share other phenotypic similarities to the *Brca2*$^{-/-}$ rat, including infertility and meiotic arrest during spermatogenesis in *Atm*$^{-/-}$ mice (Barlow *et al*., 1998). In addition, *Fancd2* homozygous knockouts display a small body type, along with abnormal meiotic chromosomal pairing during spermatogenesis (Houghtaling *et al*., 2003).

The phenotype of increased cataractogenesis in female *Brca2*$^{-/-}$ rats could also be influenced by their deficient gonadal steroid hormone production, similar to the increased risk of age-related cataracts that occurs in postmenopausal women (Klein *et al*., 1998). In a rat model for age-related cataractogenesis, estrogen replacement was protective against cataracts induced by methylnitrosourea in ovariectomized Sprague Dawley (SD) rats (Bigsby *et al*., 1999). Interestingly, estrogen treatment reduced the latency of radiation-induced cataract formation in SD rats (Dynlacht *et al*., 2006), pointing to potential differences between the etiology of age-related and radiation-associated cataracts. Insufficient gonadal steroid production must also be considered as a potential causative factor for cataractogenesis in male rats, although the effect may be androgen related. Further characterization of the *Brca2*$^{-/-}$ rat model will aid in determining if the phenotype of increased cataract formation is a primary effect from Brca2 deficiency, a secondary effect from abnormal steroidogenesis, or a combination of both factors.

In summary, this rat model provides an important opportunity to study the functions of Brca2 in late adult life by overcoming the embryonic lethality observed in similar mouse models. This increase in longevity is likely due to the unique genetic background provided by the rat. Many of the phenotypic traits we observed in *Brca2*$^{-/-}$ rats are similar to those seen in mouse models, including decreased survivability, increased cancer incidence, growth inhibition, infertility and meiotic arrest during spermatogenesis. However, the most common sites of tumor formation differ from those seen in mice with exon 11 truncating *Brca2* mutations, and the increased incidence of ocular lesions and

cataracts have not been observed in mouse models with disrupted *Brca2* function. It is also important to note that some diseases that occur naturally in aging rats, such as cataracts (Mohr *et al*., 1994) and carcinogenesis (Nakazawa *et al*., 2001), occur with higher frequency in $Brca2^{-/-}$ rats than in $Brca2^{+/-}$ or $Brca2^{+/+}$ animals, and may be related to the role of Brca2 in maintaining genomic integrity. As these studies were carried out in the outbred SD rat strain, future studies using inbred strains carrying the *Brca2* mutation will be useful in assessing the effect of genetic background on the phenotype. Additional studies will also allow us to determine if these phenotypes are directly or indirectly due to the absence of *Brca2* and to identify specific functions in novel tissues.

Materials and methods

Animals

Rats were maintained in an AALACC-approved facility and all protocols were approved through the University of Wisconsin Medical School Animal Care and Use Committee. Rats were group-housed, fed Teklad lab blox chow and acidified water *ad libitum* and maintained in a 12-h light/dark cycle.

The methods used to produce the *Brca2* knockout founder #3938 male rat have been previously published (Zan *et al*., 2003). This rat was bred to outbred SD (Harlan Sprague-Dawley, Madison, WI, USA) female rats to produce N1 pups. These N1 $Brca2^{+/-}$ carrier rats were bred to SD female rats to produce N2 pups. The N2 $Brca2^{+/-}$ carriers were bred together to produce N2 × N2 homozygous, heterozygous and littermate control rats for long-term phenotyping. Rats were assessed for tumor/cancer incidence at 24 months of age, or earlier if appearing sick or moribund. Statistical analyses of tumor/cancer incidence were carried out using Fisher's exact test with R software (http://www.r-project.org/).

Genotyping

A small tail tip section from each rat was removed at 1–4 weeks of age. Isolation of DNA was carried out as described previously (Samuelson *et al*., 2003). Genomic DNA was PCR amplified using the following primers: FP3435 5′-TCA TAA CTT AAC GCC CAG CC-3′ and RP5267 5′-AAG GCA TTT CCT GCA AAA TC-3′. A 10 μl reaction was used containing 1 × reaction buffer, 200 μM dNTPs, 2.5 ng/μl of each primer, 0.5 U Herculase and 1 μl of diluted DNA (~50–100 ng). Each reaction was denatured for 2 min at 95°C followed by 35 cycles of 92°C for 1 min, 60°C for 45 s, 72°C for 4 min and a final extension at 72°C for 7 min. PCR products were cleaned up using ExoSAP-IT. The final sequencing reaction included 4 μl of the purified PCR product and 16 μl of sequencing master mix, consisting of 1 × dilution buffer, 1 μl BigDye Terminator (Applied Biosystems), and 0.25 μM of the following primer: SEQ3997 5′-AGT AAG TGC CAG GTA ACA GTA. Each 20 μl reaction underwent an initial denaturation of 3 min at 95°C followed by 40 cycles of 95°C for 30 s, 45°C for 30 s, 52°C for 4 min, and a final extension at 72°C for 7 min. These reactions were analysed using capillary based, automated DNA sequencer platforms.

Brca2 protein expression in rat testes

Testes were collected from adult male $Brca2^{-/-}$, $Brca2^{+/-}$ and $Brca2^{+/+}$ rats. Proteins were extracted following homogenization in buffer containing 50 mM HEPES, 150 mM NaCl, 10% glycerol, 1% Triton-X 100, 10 mM EGTA, 1 mM dithiothreitol, 10 mM $Na_4P_2O_7$ and 15 mM $MgCl_2$, with phosphatase inhibitors (200 mM sodium vanadate, 100 mM NaF, 80 mM sodium-glycerolphosphate) and protease inhibitors (1 μg/ml pepstatin, 2.5 μg/ml aprotinin, 5 μg/ml leupeptin). Following centrifugation to remove debris, the total protein concentration in each extract was determined (BCA Assay, Pierce, Rockford, IL, USA). Samples were then boiled for 5 min in an equal volume of SDS sample buffer containing 10% beta-mercaptoethanol. An equal amount of total protein (100 μg) per sample was separated using sodium dodecyl sulfate–polymerase chain reaction (SDS–PAGE) on 5% acrylamide gels and electroblotted onto nitrocellulose membranes using conditions described previously (Sarkisian *et al*., 2001). Immunoblotting for Brca2 was carried out using 2 μg/ml polyclonal antiserum directed against amino acids 19–135 of mouse Brca2 (BRCA2A), provided by Lewis A Chodosh, University of Pennsylvania Cancer Center, using protocols detailed elsewhere (Sarkisian *et al*., 2001). Following incubation with a 1/3000 dilution of goat-anti-rabbit secondary antibody (Santa Cruz Biotechnology, Santa Cruz, CA, USA), the signal was detected with chemiluminescence detection reagents (Pierce) on X-ray film. Mouse testis protein extract was used as a positive control.

Estrogen replacement

Male $Brca2^{+/-}$ carriers (N3 generation) were backcrossed to female SD rats to obtain $Brca2^{+/-}$ N4 generation carriers. The backcrossing of carriers was continued until the N8 generation, where heterozygous breeding pairs were collected. Female N8 × N8 $Brca2^{-/-}$, $Brca2^{+/-}$ and $Brca2^{+/+}$ offspring ($n = 4$–6/group) were used for estrogen replacement studies. At 6 weeks of age, rats were bilaterally ovariectomized and implants containing beta-estradiol (Sigma, St Louis, MO, USA) were placed the interscapular area. Estrogen implants were prepared in 1 cm lengths of Silastic brand (i.d. 0.062″, o.d. 0.125″) (Dow Corning, Midland, MI, USA) tubing sealed with medical adhesive. This dose was previously shown to achieve circulating estradiol concentrations that approximated physiological levels for SD rats (Bigsby *et al*., 1999). After 6 weeks of estrogen replacement, animals were necropsied for analysis of mammary gland morphology. Age-matched control rats that did not undergo ovariectomy or estrogen treatment were used for comparison. Aluminum carmine-stained mammary whole mounts were prepared as previously described (Brown and Lamartiniere, 1995) and observed under light microscopy. Photographs were taken without magnification using a SONY digital camera.

Aspermatogenesis characterization

Anti-Scp3 mouse polyclonal antibodies were raised against a GST fusion of the full-length rat Scp3 protein. Anti-γH2AX antibodies were from Trevigen (Gaithersburg, MD, USA); anti-Rad 51 and anti-Dmc 1 were from Santa Cruz Biotechnology (Santa Cruz, CA, USA) (H92 and C-20, respectively). Rabbit anti-Scp1 antibody was a gift from C Hoog (Liu *et al*., 1996) and human CREST antisera was a gift from B Brinkley (Brenner *et al*., 1981). Secondary antibodies were from Jackson IR laboratories (Westgrove, PA, USA). The primary antibody were used at the following dilutions: anti-SCP3 – 1:800, anti-γH2AX – 1:100, anti-Rad51 – 1:50, anti-Dmc1 – 1:100, anti-Scp1 – 1:100, CREST antiserum – 1:500.

The protocol for meiotic chromosome spreads was modified from the procedure described by Moens *et al*., 1998. Following removal of the testicular capsule, seminiferous tubules were

finely chopped with a scalpel in RPMI 1640 high-glucose media (GIBCO-BRL, Gaithersburg, MD, USA). The cells were released from the tubules by gently pipetting in and out and filtered through a Falcon 40 μm cell strainer (BD Biosciences, San Jose, CA, USA). The suspension was centrifuged for 8 min at 800 g, the cells were resuspended in RPMI and pelleted. The pellet was resuspended in 0.5% NaCl after removal of any residual media. Cell suspension (15 μl) was added to the glass slides with hydrophobic rings (BD Biosciences, San Jose, CA, USA), and the cells were allowed to adhere without drying out for 10–15 min. Following fixation in 2% paraformaldehyde, slides were exposed to 0.03% SDS for 3 min, 2% paraformaldehyde for 3 min, washed three times in 0.4% Photo-Flo 200 (Kodak, Rochester, NY, USA) for 1 min and air dried. The slides were stored at -20°C.

For immunostaining, slides were incubated with blocking solution (10% donkey serum, 3% BSA and 0.05% Triton X-100 in PBS) for 20 min at 37°C in a humidity chamber. Primary antibodies were diluted in blocking buffer and incubated under the same conditions for 1–2 h. After two 5 min washes in 0.4% Photo-Flo/PBS solution, slides were blocked for an additional 5 min and incubated with secondary antibodies for 20 min at 37°C. The slides were washed twice with 0.4% Photo-Flo in PBS, rinsed twice with 0.4% Photo-Flo and allowed to air dry. Vectashield Mounting Medium with DAPI (Vector Laboratories, Burlingame, CA, USA) was added for coverslipping, and the slides were viewed with a Leica fluorescent microscope. Images were captured at $\times 1000$ magnification with OpenLab software and processed using Adobe Photoshop.

Evaluation of ocular pathology

At approximately 8–11 months of age, a random subset of *Brca2*$^{-/-}$, *Brca2*$^{+/-}$ and *Brca2*$^{+/+}$ rats were examined for ocular pathology using a Kowa SL-2 hand held slit lamp and ophthalmoscope. The rats were given a drop of 1% atropine in each eye to dilate the pupil/relax the lens and restrained for approximately 1–3 min for the examination. At necropsy, eyes were fixed in 10% buffered formalin and processed for embedding in paraffin. Sections (5 μm) were cut and stained with hematoxylin and eosin and viewed by light microscopy.

Acknowledgements

The authors thank Dr Ruth Sullivan (UW Research Animals Resource Center) for assistance in analyzing histopathology samples. This work was supported by the following grants, NIH CA106216 and DOD W81XWH-04-1-0436. Peti Thuwajit was supported by TRF-UW Postdoctoral Research Scholar #IPD4680004.

References

Allers T, Lichten M. (2001). Differential timing and control of noncrossover and crossover recombination during meiosis. *Cell* **106**: 47–57.

Barlow C, Liyanage M, Moens PB, Tarsounas M, Nagashima K, Brown K *et al*. (1998). Atm deficiency results in severe meiotic disruption as early as leptonema of prophase 1. *Development* **125**: 4007–4017.

Bignell G, Micklem G, Stratton MR, Ashworth A, Wooster R. (1997). The BRC repeats are conserved in mammalian BRCA2 proteins. *Hum Mol Genet* **6**: 53–58.

Bigsby RM, Cardenas H, Caperell-Grant A, Grubbs CJ. (1999). Protective effects of estrogen in a rat model of age-related cataracts. *Proc Natl Acad Sci USA* **96**: 9328–9332.

Bork P, Blomberg N, Nilges M. (1996). Internal repeats in the BRCA2 protein sequence. *Nat Genet* **13**: 22–23.

Brenner S, Pepper D, Berns MW, Tan E, Brinkley BR. (1981). Kinetochore structure, duplication, and distribution in mammalian cells: analysis by human autoantibodies from scleroderma patients. *J Cell Biol* **91**: 95–102.

Brown NM, Lamartiniere CA. (1995). Xenoestrogens alter mammary gland differentiation and cell proliferation in the rat. *Environ Health Perspect* **103**: 708–713.

Connor F, Bertwistle D, Mee PJ, Ross GM, Swift S, Grigorieva E *et al*. (1997). Tumorigenesis and a DNA repair defect in mice with a truncating Brca2 mutation. *Nat Genet* **17**: 423–430.

Cucinotta FA, Manuel FK, Jones J, Iszard G, Murrey J, Djojonegro B *et al*. (2001). Space radiation and cataracts in astronauts. *Radiat Res* **156**: 460–466.

Davies AA, Masson JY, McIlwraith MJ, Stasiak AZ, Stasiak A, Venkitaraman AR *et al*. (2001). Role of BRCA2 in control of the RAD51 recombination and DNA repair protein. *Mol Cell* **7**: 273–282.

Dobson MJ, Pearlman RE, Karaiskakis A, Spyropoulos B, Moens PB. (1994). Synaptonemal complex proteins: occurrence, epitope mapping and chromosome disjunction. *J Cell Sci* **107**: 2749–2760.

Dynlacht JR, Tyree C, Valluri S, DesRosiers C, Caperell-Grant A, Mendonca MS *et al*. (2006). Effect of estrogen on radiation-induced cataractogenesis. *Radiat Res* **165**: 9–15.

Eijpe M, Offenberg H, Goedecke W, Heyting C. (2000). Localisation of RAD50 and MRE11 in spermatocyte nuclei of mouse and rat. *Chromosoma* **109**: 123–132.

Elliott B, Jasin M. (2002). Double-strand breaks and translocations in cancer. *Cell Mol Life Sci* **59**: 373–385.

Friedman LS, Thistlethwaite FC, Patel KJ, Yu VP, Lee H, Venkitaraman AR *et al*. (1998). Thymic lymphomas in mice with a truncating mutation in Brca2. *Cancer Res* **58**: 1338–1343.

Houghtaling S, Timmers C, Noll M, Finegold MJ, Jones SN, Meyn MS *et al*. (2003). Epithelial cancer in Fanconi anemia complementation group D2 (Fancd2) knockout mice. *Genes Dev* **17**: 2021–2035.

Hunter N, Kleckner N. (2001). The single-end invasion: an asymmetric intermediate at the double-strand break to double-holliday junction transition of meiotic recombination. *Cell* **106**: 59–70.

Keeney S. (2001). Mechanism and control of meiotic recombination initiation. *Curr Top Dev Biol* **52**: 1–53.

Klein BE, Klein R, Lee KE. (1998). Incidence of age-related cataract: the Beaver Dam Eye Study. *Arch Ophthalmol* **116**: 219–225.

Liu JG, Yuan L, Brundell E, Bjorkroth B, Daneholt B, Hoog C. (1996). Localization of the N-terminus of SCP1 to the central element of the synaptonemal complex and evidence for direct interactions between the N-termini of SCP1 molecules organized head-to-head. *Exp Cell Res* **226**: 11–19.

Mahadevaiah SK, Turner JM, Baudat F, Rogakou EP, de Boer P, Blanco-Rodriguez J *et al*. (2001). Recombinational

DNA double-strand breaks in mice precede synapsis. *Nat Genet* **27**: 271–276.

McAllister KA, Bennett LM, Houle CD, Ward T, Malphurs J, Collins NK *et al*. (2002). Cancer susceptibility of mice with a homozygous deletion in the COOH-terminal domain of the Brca2 gene. *Cancer Res* **62**: 990–994.

McAllister KA, Houle CD, Malphurs J, Ward T, Collins NK, Gersch W *et al*. (2006). Spontaneous and irradiation-induced tumor susceptibility in BRCA2 germline mutant mice and cooperative effects with a p53 germline mutation. *Toxicol Pathol* **34**: 187–198.

Moens PB, Pearlman RE, Heng HH, Traut W. (1998). Chromosome cores and chromatin at meiotic prophase. *Curr Top Dev Biol* **37**: 241–262.

Mohr U, Dungworth DL, Capen CC (eds). (1994). *Pathobiology of the Aging Rat,* Vol. 2. ILSI Press: Washington, DC, 93pp.

Moynahan ME. (2002). The cancer connection: BRCA1 and BRCA2 tumor suppression in mice and humans. *Oncogene* **21**: 8994–9007.

Nakazawa M, Tawaratani T, Uchimoto H, Kawaminami A, Ueda M, Ueda A *et al*. (2001). Spontaneous neoplastic lesions in aged Sprague-Dawley rats. *Exp Anim* **50**: 99–103.

Pellegrini L, Venkitaraman A. (2004). Emerging functions of BRCA2 in DNA recombination. *Trends Biochem Sci* **29**: 310–316.

Roeder GS. (1997). Meiotic chromosomes: it takes two to tango. *Genes Dev* **11**: 2600–2621.

Samuelson DJ, Haag JD, Lan H, Monson DM, Shultz MA, Kolman BD *et al*. (2003). Physical evidence of Mcs5, a QTL controlling mammary carcinoma susceptibility, in congenic rats. *Carcinogenesis* **24**: 1445–1460.

Sarkisian CJ, Master SR, Huber LJ, Ha SI, Chodosh LA. (2001). Analysis of murine Brca2 reveals conservation of protein-protein interactions but differences in nuclear localization signals. *J Biol Chem* **276**: 37640–37648.

Schulze W, Thoms F, Knuth UA. (1999). Testicular sperm extraction: comprehensive analysis with simultaneously performed histology in 1418 biopsies from 766 subfertile men. *Hum Reprod Suppl* **1**: 82–96.

Sharan SK, Pyle A, Coppola V, Babus J, Swaminathan S, Benedict J *et al*. (2004). BRCA2 deficiency in mice leads to meiotic impairment and infertility. *Development* **131**: 131–142.

Shivji MK, Venkitaraman AR. (2004). DNA recombination, chromosomal stability and carcinogenesis: insights into the role of BRCA2. *DNA Repair (Amsterdam)* **3**: 835–843.

Siaud N, Dray E, Gy I, Gerard E, Takvorian N, Doutriaux MP. (2004). Brca2 is involved in meiosis in Arabidopsis thaliana as suggested by its interaction with Dmc1. *Embo J* **23**: 1392–1401.

Villeneuve AM, Hillers KJ. (2001). Whence meiosis? *Cell* **106**: 647–650.

Worgul BV, David J, Odrich S, Merriam Jr GR, Medvedovsky C, Merriam JC *et al*. (1991). Evidence of genotoxic damage in human cataractous lenses. *Mutagenesis* **6**: 495–499.

Worgul BV, Smilenov L, Brenner DJ, Junk A, Zhou W, Hall EJ. (2002). Atm heterozygous mice are more sensitive to radiation-induced cataracts than are their wild-type counterparts. *Proc Natl Acad Sci USA* **99**: 9836–9839.

Yoshida K, Miki Y. (2004). Role of BRCA1 and BRCA2 as regulators of DNA repair, transcription, and cell cycle in response to DNA damage. *Cancer Sci* **95**: 866–871.

Zan Y, Haag JD, Chen KS, Shepel LA, Wigington D, Wang YR *et al*. (2003). Production of knockout rats using ENU mutagenesis and a yeast-based screening assay. *Nat Biotechnol* **21**: 645–651.

Zhoucun A, Zhang S, Yang Y, Ma Y, Zhang W, Lin L. (2006). The common variant N372 H in BRCA2 gene may be associated with idiopathic male infertility with azoospermia or severe oligozoospermia. *Eur J Obstet Gynecol Reprod Biol* **124**: 61–64.

Zickler D, Kleckner N. (1999). Meiotic chromosomes: integrating structure and function. *Annu Rev Genet* **33**: 603–754.

Zierhut D, Lohr F, Schraube P, Huber P, Wenz F, Haas R *et al*. (2000). Cataract incidence after total-body irradiation. *Int J Radiat Oncol Biol Phys* **46**: 131–135.

Genetically engineered rat models for breast cancer

Bart M. G. Smits, Michelle S. Cotroneo, Jill D. Haag, and Michael N. Gould*

McArdle Lab for Cancer Research, University of Wisconsin – Madison, Madison, WI 53706, USA

*Corresponding author:
Dr. Michael N. Gould
McArdle Lab for Cancer Research, Rm 506A
University of Wisconsin – Madison
Madison, WI 53706
Tel.: +1 608 263 6615
Fax.: +1 608 262 2824
E-mail: gould@oncology.wisc.edu

Abstract

Rat mammary cancers generally resemble many features of human breast cancer. With the recent developments in rat genetic engineering, the rat has become an excellent model system to study aspects of the molecular etiology of breast cancer. In this review, we describe the efforts to generate genetically engineered rat models for breast cancer.

Introduction

Historically, rat breast cancer models have been mostly limited to chemical carcinogenesis models, as the mammary tumors resemble many aspects of human breast cancer. Rat mammary cancers, similar to human breast cancers, display a wide spectrum of responses to hormonal therapy [1]. Both rat and human mammary cancers frequently are hormone dependent, while murine mammary tumors are virtually all hormone independent [2]. In addition, chemically induced rat mammary tumors are of ductal origin, just like human breast cancers [3].

Proto-oncogenes such as *neu* and *ras* are frequently overexpressed in primary human breast cancer, whereas affecting mutations in tumor suppressor genes such as *BRCA1* and *BRCA2* underlie high-penetrance susceptibility to breast cancer. However, studies concerning the involvement of these genes in the molecular etiology of breast cancer have resulted in contradictory data. Given the strong similarity between mammary cancer in certain rat models and many aspects of human breast cancer, the rat is potentially an excellent experimental model organism to assess the role of genes such as *ras*, *neu*, *Brca1*, and *Brca2* in mammary carcinogenesis. To this end, genetic engineering in the rat or rat mammary gland needs to be employed. Transgenic overexpression models could be used to study the effect of proto-oncogenes, such as *ras* and *neu*, while the effect of tumor suppressors, such as *Brca1* and *Brca2* could be mimicked by knockout models.

The rat has historically been employed as a model organism by physiologists, whereas the mouse has always been favored by mammalian geneticists. As a result, genetic strategies to manipulate the genome are widely established for the mouse, but lag slightly behind for the rat. Recently, however, several groups have reported major advances in the genetic manipulation of the rat, which has enhanced the possibilities to utilize genetic rat models to study many facets of human health and disease [4, 5].

Transgenic rat models for breast cancer

Although many mouse models have been generated to study gain-of-function effects of proto-oncogenes and loss-of-function effects of tumor suppressors [6], transgenic rat models for breast cancer are relatively scarce. Nevertheless, many other transgenic rat models were found to relate closer to human disease than transgenic mice harboring the same transgenic constructs [7]. Transgenic technology for the rat has been available since the 1990s [8]. Via pronuclear microinjection a transgene is introduced in a fertilized oocyte. Tandem copies of the construct could randomly integrate at a single site in the genome. Successfully injected embryos are placed back into the oviduct of a pseudopregnant surrogate mother by microsurgery, and subsequent progeny are screened for the presence of the transgene by Southern Blot analysis. Since genome integration of the transgenic construct in this procedure is a random event, elucidation of the integration site is generally required.

Many breast cancers have been shown to overexpress proto-oncogenes, of which *neu* (also known as *Her2* or *c-ErbB-2*) and *ras* are the most prominent. However, the effect of overexpression of these proto-oncogenes in the molecular etiology of breast cancer remains largely unknown. A small number of overexpression models have been made to study these effects in the rat.

Transgenic rat models of neu *(*Her2 */ c*-ErbB-*2) overexpression*

An important role of Neu in primary breast cancer was implicated from the observation that the *neu* proto-oncogene is over expressed in 20%-30% of human breast cancers [9, 10], which was correlated to an increase of the aggressiveness of the tumor [11]. The *neu* gene encodes a member of the tyrosine kinase growth factor receptor family [12, 13] that upon hetero- or homodimerization mediates signal transduction. Several transgenic mouse models have been generated that express an activated form of Neu under control of the Molony mammary tumor virus (MMTV) promoter. While these mice developed mammary carcinomas that histologically resemble human tumors [14], comparable activating mutations in human breast cancer have not been found yet [10, 15]. A mouse model overexpressing rat wild type *neu* under control of the MMTV promoter also

showed development of mammary carcinomas of which many metastasized [16]. Resequencing of the transgene revealed sporadic, potentially activating mutations in the carcinoma, but not in the adjacent normal tissue [17]. Again, corresponding mutations in human breast tumors have not been found. Additionally, the carcinomas were estrogen receptor (ER)-negative and primarily resembled the infrequently occurring lobular and alveolar malignancies in humans [17].

Davies *et al.* [18] generated transgenic Sprague-Dawley (SD) rats harboring the human *neu* proto-oncogene under control of the MMTV promoter. Transgene expression is not measurable in the mammary glands of virgin rats, but is detectable in mammary tissue from mid-pregnant rats. A high percentage of the transgenic female rats developed focal hyperplastic and benign lesions, after being subjected to several cycles of pregnancy. These lesions included lobular and ductal hyperplasias, fibroadenomas, cystic expansions, and papillary adenomas. In addition, real malignancies, including Ductal Carcinoma In Situ (DCIS) and carcinoma, developed stochastically, which recapitulates the hypothesis that overexpression of the human *neu* proto-oncogene predisposes to mammary carcinogenesis. All transgenic female mammary glands failed to fully involute after lactation.

In order to generate an animal model to further explore the carcinogenic potential of overexpressed wild type *neu*, Watson *et al*. [19] generated a transgenic SD rat model expressing the rat *neu* proto-oncogene driven under the MMTV promoter. In contrast to Davies *et al.*, virgin female rats did have an elevated expression level of the transgene in the mammary gland. Interestingly, mammary carcinomas arose only when the transgenic female rats were treated with androgens (i.e. testosterone). Male transgenic animals developed mammary carcinomas in an androgen-dependent fashion. These tumors were androgen receptor (AR) positive, but negative for the ER and progesterone receptor (PR). In addition, no activating mutations in the *neu* transgene were found. Gonadoectomized rats did not develop mammary cancer, suggesting a pivotal role of androgens in the etiology of mammary carcinogenesis in the presence of *neu* overexpression. This model could potentially lead to greater understanding of the mechanisms underlying mammary carcinogenesis associated with Neu overexpression in both men and postmenopausal women.

Transgenic rat models of ras *overexpression*

Mutationally activated *ras* is associated with ~40% of human cancers, however, it is rarely observed in breast cancers [20, 21]. Overexpression of the proto-oncogene *ras* has been observed frequently in human breast cancer [22-24], and has been clinically associated with cancer progression [25-27] and unfavorable disease prognosis [28-30]. The three mammalian *ras* genes encode for Harvey (H-)RAS, Kirsten 2A (K2A-) RAS, Kirsten 2B (K2B-) RAS and N-RAS that belong to the small GTP-ase protein family. Small GTP-ases transmit signals from the receptor tyrosine kinases to the nucleus through multiple effectors pathways, such as the RAF/MEK/MAPK signaling cascade. In a mouse model overexpressing oncogenic v-Ha-*ras* under control of the MMTV promoter, mammary hyperplasias, mammary adenocarcinomas, and metastasis arose rapidly, as early as five weeks of age [31].

It is evident that activated *ras* harbors tremendous oncogenic capabilities. However, the role of overexpressed wild type *ras* in the etiology of breast cancer is poorly understood. In transgenic overexpression rat models of the rat Harvey and Kirsten *ras* genes, both under control of the rat Harvey *ras* promoter and regulatory elements, no abnormal mammary pathology was observed [32]. However, when these rats were treated with the mammary carcinogen nitrosomethylurea (NMU), an inhibition of NMU-induced mammary tumor multiplicity was observed. This is slightly surprising, since overexpression of the human form of Harvey *ras* under control of the truncated human Harvey *ras* promoter rendered the rats highly susceptible to NMU-induced mammary carcinogenesis [33, 34]. This discrepancy might illustrate the delicate role of the regulation of the Harvey *ras* gene in mammary carcinogenesis or perhaps cancer prevention, independent of an elevated frequency of activating mutations.

Infusion model

Due to the lack of embryonic stem (ES) cell-based technology for the rat, conditional knockins commonly used for time- and tissue-specific transgene expression in the mouse,

are not available. Consequently, germ line transgenesis in the rat is limited to the conventional pronuclear injection method that results in random integration of the transgene, as described above. In these models, ectopic expression of the transgene could occur due to unforeseen integration into an enhancer or repressor site in the genome. Additionally, the phenotype under study could be altered by developmental influences, since transgene (over)expression could be present already early in development, depending on the promoter. To circumvent these drawbacks Gould and coworkers developed a mammary duct infusion model for the rat [35]. This technology allows for the direct anatomical targeting of the mammary ductal epithelial cells with transgenic constructs via retroviral vectors. Since the retroviral vector can only integrate into the genome of proliferating cells, the technology is very specific to mammary epithelial cells, if delivered at the appropriate developmental stage (~50-55 days of age). By varying the virus titer any percentage of cells can be targeted, which makes it a flexible experimental system.

The major advantage of the infusion model is the relative rapidity of the procedure. The method does not rely on zygote manipulation, but on simply cloning the desired transgene in the replication-defective retroviral vector.

Infusion of neu

The infusion of oncogenic *neu* under control of the MMTV long terminal repeat (LTR) directly into the mammary ducts of female rats resulted in full penetrance development of mammary carcinomas [35]. The carcinomas resulted from single cell transformations [36]. Tumor development strongly overlapped with the various stages in human breast cancer [37], although a general classification system, as is available for mammary carcinogenesis in genetically engineered mice [38], has not been generated for rat mammary carcinogenesis yet. Between two and seven weeks after infusion the first cribiform- (Fig. 1b) and comedo-like (Fig. 1c) hyperplastic structures appeared that resemble DCIS observed in early human breast cancer. These hyperplasias further developed into invasive carcinomas (Fig. 1d).

A large portion of the carcinomas (~50%-60%) responded to hormone ablation by ovariectomy [1] or can be prevented by treatment with the antiestrogenic drug tamoxifen

[39]. Tamoxifen treatment also prevents ~50% of invasive breast cancer in women [40], again illustrating the relevance of the rat *neu* infusion model to human breast cancer and more specifically chemoprevention.

Infusion of ras

Although the expression difference between the members of the Ras family in the mammary gland was reported to be modest (1.5 - 2 fold), it appeared that activated Harvey *ras* is an order of magnitude more potent at inducing mammary carcinomas when infused directly into the mammary duct, compared to activated Kirsten *ras* [41]. This modest expression difference is unlikely to account for the large difference in oncogenic potential. Thus, the rat mammary duct infusion model was further employed to characterize the carcinogenic potential of the regions that differ between Harvey *ras* and Kirsten *ras*. By infusing Harvey and Kirsten *ras* chimaeras, regions that are important to the carcinogenic potential of Harvey *ras* in the mammary duct were determined [42]. These regions could potentially account for the tissue-specific differences of the carcinogenic potential of activated *ras* isoforms.

In addition, the wild type form of Harvey *ras*, but not Kirsten *ras*, under control of the MMTV promoter resulted in mammary carcinomas when directly infused into the mammary duct [42]. This is in contrast to the germ line transgenic overexpression rat model of the proto-oncogene Harvey *ras* under control of its own promoter that caused resistance to NMU-induced carcinogenesis [32]. Possibly, gene regulation through the distinct promoters could be inherent to this discrepancy. Taken together, these data suggest a delicate interplay of *ras* expression, activation, and protein composition in the tissue- and time-specific carcinogenic potential of the *ras* isoforms that requires further study.

Rat knockout models for BRCA1 and BRCA2

Between 2% and 3% of human breast cancer cases are associated with mutations in *BRCA1* or *BRCA2* [43, 44]. Individuals carrying inactivating mutations in these genes are

highly susceptible to developing breast cancer. Their lifetime risk is estimated to be up to 80% [45]. Frequently, cancer initiation in these patients is caused by loss of heterozygosity [46, 47]. This mechanism results in the loss of the wild type allele in a cell, which totally abolishes normal BRCA1 or BRCA2 protein expression.

Rat models for breast cancers often accurately reflect human breast cancer in terms of hormone responsiveness and the ductal origin of the lesion [2, 3]. However, the motivation for generating rat knockout models for *Brca1* and *Brca2* is hampered by the lack of ES cell-based knockout technology. Therefore, gene inactivation technology based on chemical germ line mutagenesis was recently developed for the rat [48, 49].

Briefly, male rats are mutagenized using the germ line mutagen *N*-ethyl-*N*-nitrosourea (ENU), which induces random point mutations in the sperm cells with relative high frequency. Mating these males to untreated females results in progeny that carry random heterozygous point mutations in their genome. Various high-throughput mutation discovery platforms have been used to retrieve these heterozygous mutations in genes of interest [48-50]. The first rat knockouts produced via this technology were the *Brca1* and *Brca2* knockouts [49].

Phenotype of Brca1 *and* Brca2 *mutant rats*

The $Brca1^{+/-}$ mutant founder generated through ENU mutagenesis produced viable and fertile heterozygous male and female carriers, however, intercross of these carriers failed to produce pups that were homozygous for the mutation (J. D. H. and M. N. G., unpublished). This finding was not surprising, as embryonic lethality or limited survival is commonly observed for most mouse *Brca1* and *Brca2* mutants when homozygous [51]. In contrast, the *Brca2* mutation showed normal Mendelian inheritance in the rat when bred to homozygosity, with 100% viability of $Brca2^{-/-}$ offspring [49]. Full length Brca2 protein was identified from testicular extracts from $Brca2^{+/+}$ and $Brca2^{+/-}$ rats, and was absent in $Brca2^{-/-}$ testes, providing validation of this model and a unique opportunity to assess Brca2-associated breast cancer susceptibility [52].

Phenotypic evaluation of $Brca2^{-/-}$ rats having the SD genetic background revealed several abnormalities [52]. Compared with $Brca2^{+/+}$ and $Brca2^{+/-}$ littermates, $Brca2^{-/-}$ rats were significantly smaller and were infertile, as a consequence of impaired gonad

development. The mammary glands of female rats were underdeveloped, most likely because of insufficient production of ovarian hormones. Long-term phenotypic assessment showed increased cataractogenesis and shortened lifespan in both male and female *Brca2*$^{-/-}$ rats, which was due to formation of a variety of tumors and carcinomas. The most frequently occurring lesion in *Brca2*$^{-/-}$ rats was osteosarcoma, differing from mouse knockouts, which had a high incidence of thymic lymphoma [51]. These lesions do not reflect the tumor spectrum of human *BRCA2* mutation carriers, for which the major sites of cancer are the breast, ovary and prostate. As the frequency of spontaneous mammary carcinomas in *Brca2*$^{-/-}$ rats did not differ from controls, additional methods were needed to establish a breast cancer model.

Strategies for mammary carcinoma induction in Brca2$^{-/-}$ *rats*

The lack of gonad development in *Brca2*$^{-/-}$ rats presented a major obstacle for establishing a breast cancer model, as the growth of most rat mammary carcinomas requires ovarian hormones. The underdeveloped mammary glands of *Brca2*$^{-/-}$ female rats are estrogen responsive, as short-term estrogen replacement using implants following ovariectomy induced ductal elongation and branching morphogenesis [52]. Since it is difficult to mimic normal ovarian hormone secretion in a long-term fashion to allow for mammary carcinoma development, other methods were needed to correct the ovarian defect in *Brca2*$^{-/-}$ rats.

In an unpublished study, the *Brca2* mutation was moved to the Wistar-Furth (WF) genetic background (M. S. C. and M. N. G., unpublished). This provides the alternative of using tissue transplantation models to assess mammary carcinogenesis, as graft rejection can be circumvented using inbred strains. The *Brca2*$^{-/-}$ WF rats are phenotypically similar to their *Brca2*$^{-/-}$ SD counterparts; they are small and infertile, with underdeveloped gonads and mammary glands. Therefore, providing a normal hormonal environment for the developing *Brca2*$^{-/-}$ mammary gland could theoretically be achieved by transplanting normal ovaries into *Brca2*$^{-/-}$ rats, or by transplanting *Brca2*$^{-/-}$ mammary glands into wild type hosts. Surgical transplantation of *Brca2*$^{+/+}$ ovaries into the subscapular fat pads of four-week-old ovariectomized *Brca2*$^{-/-}$ recipients showed initial success, as estrus cycling could be observed 6-10 weeks following surgery. However,

long-term viability of the transplanted ovaries was poor, and *Brca2*$^{-/-}$ rats failed to develop mammary carcinomas after 6-11 months, possibly due to disruption of normal hypothalamic-pituitary-ovarian feedback.

Providing a normal hormonal setting for the *Brca2*$^{-/-}$ mammary gland by transplant into the subscapular fat pads of *Brca2*$^{+/+}$ recipients was an attractive alternative, as hosts did not require ovariectomy. In general, the *Brca2*$^{-/-}$ mammary transplants had a higher degree of branching and lobularity than control transplants from *Brca2*$^{+/+}$ donors (Table 1; Fig. 2). Despite the seemingly accelerated growth of *Brca2*$^{-/-}$ transplants, mammary carcinomas failed to develop after a one year period (Table 1). Nonetheless, the *Brca2*$^{-/-}$ mammary gland is likely to have increased responsiveness to prolactin or progesterone, as these hormones play a major role in lobular growth and differentiation.

Mammary cancer susceptibility in Brca1$^{+/-}$ *and* Brca2$^{+/-}$ *rats*

Brca1$^{+/-}$ (n=9) and *Brca1*$^{+/+}$ controls (n=14) were evaluated over a one year period for spontaneous tumor/cancer formation, however, neither mammary nor any other carcinomas were found (J.D.H. and M.N.G., unpublished). Similarly, *Brca2*$^{+/-}$ carriers had very low spontaneous cancer/tumor incidence, which did not differ significantly from *Brca2*$^{+/+}$ littermates [52]. Likewise, mouse *Brca1*$^{+/-}$ and *Brca2*$^{+/-}$ carriers do not show increased tumor susceptibility [51]. The discrepancy between high tumor incidence in human carriers of *BRCA1* and *BRCA2* mutations and the rodent heterozygous mutant phenotype could be due to a lack of haploinsufficiency or very long latency in these rodent models. In an attempt to shorten the latency in *Brca2*$^{+/-}$ carrier rats chemical carcinogens *7,12*-dimethylbenz[a]anthracene (DMBA) or NMU were administered. However, these carcinogens failed to increase mammary carcinoma multiplicity compared to wild type littermates (M.S.C. and M.N.G., unpublished). Interestingly, attempts to model cancer in *Brca2*$^{+/-}$ mice by treatment with DMBA and medroxyprogesterone acetate actually increased mammary tumor latency in carriers compared with wild type littermates controls [53]. These contradictory phenotypes in response to treatment with chemical carcinogens point to the existence of species-specific modifiers that affect the role of *Brca2* in carcinogenesis.

Conclusions

Rat models for breast cancer are of great interest since the origin, pathology, and sensitivity to hormones of rat mammary tumors closely resemble those of the human [2, 3]. The mouse has always been the model organism of choice for mammalian geneticists, but with the recent developments in the field of rat genetics and genomics, the rat is clearly gaining status as a genetic model organism [4, 5, 54]. Here we reviewed the efforts to establish genetically engineered rat models for breast cancer (overview in Table 2).

The transgenic and infusion models of *neu* and *ras* illustrate that genetically engineered rat models are comprehensive model systems to study certain aspects of the etiology of human breast cancer. The differences in susceptibility to mammary carcinogenesis in the various transgenic rat models suggest that not mutational activation, but aberrant regulation of the expression of the proto-oncogenes *neu* and *ras* could account for that. Although the activated forms of *neu* and *ras* are infrequent in human breast cancer, they do provide an excellent opportunity to induce mammary carcinomas with high frequency when infused directly into the mammary duct. In addition, mammary carcinomas induced by the retroviral infusion of activated *neu* result in DCIS-like hyperplasias that develop into frank carcinomas. A large portion of these mammary cancers are hormone responsive, just like human breast cancer, which makes this model highly relevant for chemoprevention studies [39].

The rationale for producing genetically engineered rodents having mutant copies of tumor suppressor genes like *Brca1* and *Brca2* is to model the human cancers that arise from mutations in these genes. However, these mutations in heterozygous state fail to result in increased breast cancer susceptibility in mice and rats, even when additional DNA damage is induced with mammary carcinogens. Importantly, the rat *Brca2* knockout model provided the distinct advantage of viability in the homozygous state, but mammary carcinomas did not arise spontaneously. Even providing the *Brca2*$^{-/-}$ mammary gland with a normal hormonal environment to test for ovarian insufficiency in these homozygous knockouts did not result in tumor formation. Despite the tremendous efforts

to develop these unique knockout models into breast cancer models, the utility of these models lies in the ability to study the tissue-specific functions of the proteins.

It is worth mentioning that another ENU-induced rat cancer model described recently does recapitulate the human disease better than the existing murine models. In this case, the rat Adenomatous polyposis coli (*Apc*) heterozygous knockouts develop multiple large neoplasms distributed between the colon and the small intestine [55], whereas the mouse carriers of the mutant *Apc* allele primarily have a small intestine phenotype [56]. This example illustrates that rat knockout models could potentially provide enhanced model systems to study aspects of human familial cancer.

Interestingly, the rat models reviewed here display a dynamic range of mammary phenotypes when compared to each other and to existing murine models. Some models develop carcinomas, others develop carcinomas only if treated with a carcinogen or hormones, while others don't develop mammary cancer at all. The phenotypic outcome of a genetically engineered model could be influenced by environmental factors, such as animal housing, food, and mode of carcinogen administration, and/or genetic factors.

The genetic influences can be categorized in two groups. First, local genetic elements are an important factor to consider when analyzing a mutant phenotype. Such genetic elements include the promoter driving transgene expression, the site of integration of a transgenic construct, the nature of the genetic alteration of the gene of interest, and more. Second, genome-wide genetic influences, i.e. the genetic background of the strain in which the genetic alteration is induced, could be a major influence. Strain effects on mammary carcinogenesis susceptibility have been described previously for transgenic *neu* proto-oncogene-induced mouse models [57] and have recently been documented for a rat oncogenic *neu* infusion experiment [58].

Finally, certain genes could have a different role in the mammary gland of different species, which makes interspecies comparison of genetically engineered models virtually impossible, like the *Brca2* models described in this review. Therefore, each model designed to simulate specific aspects of human breast cancer should be considered as a separate experiment with its own controls and results. In that perspective, the rat models described in this review clearly have an additive value to the existing genetically

engineered models, such as mice and human cells, to study specific aspects of human breast cancer.

Acknowledgements

B. M. G. S. is supported by a Rubicon grant from the Netherlands Organisation for Scientific Research (NWO). This work was supported by the following grants, NIH CA106216 and DOD W81XWH-04-1-0436.

References

[1] B. Wang, W.S. Kennan, J. Yasukawa-Barnes, M.J. Lindstrom, and M.N. Gould, Difference in the response of neu and ras oncogene-induced rat mammary carcinomas to early and late ovariectomy, *Cancer Res* 52 (1992), 4102-4105

[2] S. Nandi, R.C. Guzman, and J. Yang, Hormones and mammary carcinogenesis in mice, rats, and humans: a unifying hypothesis, *Proc Natl Acad Sci U S A* 92 (1995), 3650-3657

[3] J. Russo, B.A. Gusterson, A.E. Rogers, I.H. Russo, S.R. Wellings, and M.J. van Zwieten, Comparative study of human and rat mammary tumorigenesis, *Lab Invest* 62 (1990), 244-278

[4] J. Lazar, C. Moreno, H.J. Jacob, and A.E. Kwitek, Impact of genomics on research in the rat, *Genome Res* 15 (2005), 1717-1728

[5] B.M. Smits, and E. Cuppen, Rat genetics: the next episode, *Trends Genet* 22 (2006), 232-240

[6] Q. Shen, and P.H. Brown, Transgenic mouse models for the prevention of breast cancer, *Mutat Res* 576 (2005), 93-110

[7] B. Charreau, L. Tesson, J.P. Soulillou, C. Pourcel, and I. Anegon, Transgenesis in rats: technical aspects and models, *Transgenic Res* 5 (1996), 223-234

[8] L.J. Mullins, G. Brooker, and J.J. Mullins, Transgenesis in the rat, *Methods Mol Biol* 180 (2002), 255-270

[9] D.J. Slamon, G.M. Clark, S.G. Wong, W.J. Levin, A. Ullrich, and W.L. McGuire, Human breast cancer: correlation of relapse and survival with amplification of the HER-2/neu oncogene, *Science* 235 (1987), 177-182

[10] D.J. Slamon, W. Godolphin, L.A. Jones, J.A. Holt, S.G. Wong, D.E. Keith, W.J. Levin, S.G. Stuart, J. Udove, A. Ullrich, and et al., Studies of the HER-2/neu proto-oncogene in human breast and ovarian cancer, *Science* 244 (1989), 707-712

[11] D.J. Slamon, B. Leyland-Jones, S. Shak, H. Fuchs, V. Paton, A. Bajamonde, T. Fleming, W. Eiermann, J. Wolter, M. Pegram, J. Baselga, and L. Norton, Use of chemotherapy plus a monoclonal antibody against HER2 for metastatic breast cancer that overexpresses HER2, *N Engl J Med* 344 (2001), 783-792

[12] L. Coussens, T.L. Yang-Feng, Y.C. Liao, E. Chen, A. Gray, J. McGrath, P.H. Seeburg, T.A. Libermann, J. Schlessinger, U. Francke, and et al., Tyrosine kinase receptor with extensive homology to EGF receptor shares chromosomal location with neu oncogene, *Science* 230 (1985), 1132-1139

[13] P.P. Di Fiore, J.H. Pierce, M.H. Kraus, O. Segatto, C.R. King, and S.A. Aaronson, erbB-2 is a potent oncogene when overexpressed in NIH/3T3 cells, *Science* 237 (1987), 178-182

[14] J.N. Hutchinson, and W.J. Muller, Transgenic mouse models of human breast cancer, *Oncogene* 19 (2000), 6130-6137

[15] N.R. Lemoine, S. Staddon, C. Dickson, D.M. Barnes, and W.J. Gullick, Absence of activating transmembrane mutations in the c-erbB-2 proto-oncogene in human breast cancer, *Oncogene* 5 (1990), 237-239

[16] C.T. Guy, M.A. Webster, M. Schaller, T.J. Parsons, R.D. Cardiff, and W.J. Muller, Expression of the neu protooncogene in the mammary epithelium of transgenic mice induces metastatic disease, *Proc Natl Acad Sci U S A* 89 (1992), 10578-10582

[17] P.M. Siegel, D.L. Dankort, W.R. Hardy, and W.J. Muller, Novel activating mutations in the neu proto-oncogene involved in induction of mammary tumors, *Mol Cell Biol* 14 (1994), 7068-7077

[18] B.R. Davies, A.M. Platt-Higgins, G. Schmidt, and P.S. Rudland, Development of hyperplasias, preneoplasias, and mammary tumors in MMTV-c-erbB-2 and MMTV-TGFalpha transgenic rats, *Am J Pathol* 155 (1999), 303-314

[19] P.A. Watson, K. Kim, K.S. Chen, and M.N. Gould, Androgen-dependent mammary carcinogenesis in rats transgenic for the Neu proto-oncogene, *Cancer Cell* 2 (2002), 67-79

[20] J.L. Bos, ras oncogenes in human cancer: a review, *Cancer Res* 49 (1989), 4682-4689

[21] S. Miyakis, G. Sourvinos, and D.A. Spandidos, Differential expression and mutation of the ras family genes in human breast cancer, *Biochem Biophys Res Commun* 251 (1998), 609-612

[22] T. Clair, W.R. Miller, and Y.S. Cho-Chung, Prognostic significance of the expression of a ras protein with a molecular weight of 21,000 by human breast cancer, *Cancer Res* 47 (1987), 5290-5293

[23] G.J. Clark, and C.J. Der, Aberrant function of the Ras signal transduction pathway in human breast cancer, *Breast Cancer Res Treat* 35 (1995), 133-144

[24] M.E. DeBortoli, H. Abou-Issa, B.E. Haley, and Y.S. Cho-Chung, Amplified expression of p21 ras protein in hormone-dependent mammary carcinomas of humans and rodents, *Biochem Biophys Res Commun* 127 (1985), 699-706

[25] P.H. Hand, A. Thor, D. Wunderlich, R. Muraro, A. Caruso, and J. Schlom, Monoclonal antibodies of predefined specificity detect activated ras gene expression in human mammary and colon carcinomas, *Proc Natl Acad Sci U S A* 81 (1984), 5227-5231

[26] J. Lundy, R. Grimson, Y. Mishriki, S. Chao, S. Oravez, F. Fromowitz, and M.V. Viola, Elevated ras oncogene expression correlates with lymph node metastases in breast cancer patients, *J Clin Oncol* 4 (1986), 1321-1325

[27] N. Ohuchi, A. Thor, D.L. Page, P.H. Hand, S.A. Halter, and J. Schlom, Expression of the 21,000 molecular weight ras protein in a spectrum of benign and malignant human mammary tissues, *Cancer Res* 46 (1986), 2511-2519

[28] C. Dati, R. Muraca, O. Tazartes, S. Antoniotti, I. Perroteau, M. Giai, P. Cortese, P. Sismondi, G. Saglio, and M. De Bortoli, c-erbB-2 and ras expression levels in breast cancer are correlated and show a co-operative association with unfavorable clinical outcome, *Int J Cancer* 47 (1991), 833-838

[29] U.J. Gohring, T. Schondorf, V.R. Kiecker, M. Becker, C. Kurbacher, and A. Scharl, Immunohistochemical detection of H-ras protooncoprotein p21 indicates favorable prognosis in node-negative breast cancer patients, *Tumour Biol* 20 (1999), 173-183

[30] D.M. Watson, R.A. Elton, W.J. Jack, J.M. Dixon, U. Chetty, and W.R. Miller, The H-ras oncogene product p21 and prognosis in human breast cancer, *Breast Cancer Res Treat* 17 (1991), 161-169

[31] E. Sinn, W. Muller, P. Pattengale, I. Tepler, R. Wallace, and P. Leder, Coexpression of MMTV/v-Ha-ras and MMTV/c-myc genes in transgenic mice: synergistic action of oncogenes in vivo, *Cell* 49 (1987), 465-475

[32] T.A. Thompson, J.D. Haag, and M.N. Gould, ras gene mutations are absent in NMU-induced mammary carcinomas from aging rats, *Carcinogenesis* 21 (2000), 1917-1922

[33] M. Asamoto, T. Ochiya, H. Toriyama-Baba, T. Ota, T. Sekiya, M. Terada, and H. Tsuda, Transgenic rats carrying human c-Ha-ras proto-oncogenes are highly susceptible to N-methyl-N-nitrosourea mammary carcinogenesis, *Carcinogenesis* 21 (2000), 243-249

[34] H. Tsuda, M. Asamoto, T. Ochiya, H. Toriyama-Baba, A. Naito, T. Ota, T. Sekiya, and M. Terada, High susceptibility of transgenic rats carrying the human c-Ha-ras proto-oncogene to chemically-induced mammary carcinogenesis, *Mutat Res* 477 (2001), 173-182

[35] B. Wang, W.S. Kennan, J. Yasukawa-Barnes, M.J. Lindstrom, and M.N. Gould, Frequent induction of mammary carcinomas following neu oncogene transfer into in situ mammary epithelial cells of susceptible and resistant rat strains, *Cancer Res* 51 (1991), 5649-5654

[36] Y.T. Tai, and M.N. Gould, The genetic penetrance of the activated neu oncogene for the induction of mammary cancer in vivo, *Oncogene* 14 (1997), 2701-2707

[37] M.N. Gould, The introduction of activated oncogenes to mammary cells in vivo using retroviral vectors: a new model for the chemoprevention of premalignant and malignant lesions of the breast, *J Cell Biochem Suppl* 17G (1993), 66-72

[38] R.D. Cardiff, M.R. Anver, B.A. Gusterson, L. Hennighausen, R.A. Jensen, M.J. Merino, S. Rehm, J. Russo, F.A. Tavassoli, L.M. Wakefield, J.M. Ward, and J.E. Green, The mammary pathology of genetically engineered mice: the consensus report and recommendations from the Annapolis meeting, *Oncogene* 19 (2000), 968-988

[39] S. Woditschka, J.D. Haag, J.L. Waller, D.M. Monson, A.A. Hitt, H.L. Brose, R. Hu, Y. Zheng, P.A. Watson, K. Kim, M.J. Lindstrom, B. Mau, V.E. Steele, R.A. Lubet, and M.N. Gould, Neu-induced retroviral rat mammary carcinogenesis: a novel chemoprevention model for both hormonally responsive and nonresponsive mammary carcinomas, *Cancer Res* 66 (2006), 6884-6891

[40] B. Fisher, J.P. Costantino, D.L. Wickerham, C.K. Redmond, M. Kavanah, W.M. Cronin, V. Vogel, A. Robidoux, N. Dimitrov, J. Atkins, M. Daly, S. Wieand, E. Tan-Chiu, L. Ford, and N. Wolmark, Tamoxifen for prevention of breast cancer: report of the

National Surgical Adjuvant Breast and Bowel Project P-1 Study, *J Natl Cancer Inst* 90 (1998), 1371-1388

[41] T.A. Thompson, K. Kim, and M.N. Gould, Harvey ras results in a higher frequency of mammary carcinomas than Kirsten ras after direct retroviral transfer into the rat mammary gland, *Cancer Res* 58 (1998), 5097-5104

[42] K. Kim, M.J. Lindstrom, and M.N. Gould, Regions of H- and K-ras that provide organ specificity/potency in mammary cancer induction, *Cancer Res* 62 (2002), 1241-1245

[43] W.D. Foulkes, Polygenic or pollyanna?, *Nat Med* 8 (2002), 328-330

[44] K.L. Nathanson, and B.L. Weber, "Other" breast cancer susceptibility genes: searching for more holy grail, *Hum Mol Genet* 10 (2001), 715-720

[45] S.A. Narod, and W.D. Foulkes, BRCA1 and BRCA2: 1994 and beyond, *Nat Rev Cancer* 4 (2004), 665-676

[46] N. Collins, R. McManus, R. Wooster, J. Mangion, S. Seal, S.R. Lakhani, W. Ormiston, P.A. Daly, D. Ford, D.F. Easton, and et al., Consistent loss of the wild type allele in breast cancers from a family linked to the BRCA2 gene on chromosome 13q12-13, *Oncogene* 10 (1995), 1673-1675

[47] S.A. Smith, D.F. Easton, D.G. Evans, and B.A. Ponder, Allele losses in the region 17q12-21 in familial breast and ovarian cancer involve the wild-type chromosome, *Nat Genet* 2 (1992), 128-131

[48] B.M. Smits, J. Mudde, R.H. Plasterk, and E. Cuppen, Target-selected mutagenesis of the rat, *Genomics* 83 (2004), 332-334

[49] Y. Zan, J.D. Haag, K.S. Chen, L.A. Shepel, D. Wigington, Y.R. Wang, R. Hu, C.C. Lopez-Guajardo, H.L. Brose, K.I. Porter, R.A. Leonard, A.A. Hitt, S.L. Schommer, A.F. Elegbede, and M.N. Gould, Production of knockout rats using ENU mutagenesis and a yeast-based screening assay, *Nat Biotechnol* 21 (2003), 645-651

[50] B.M. Smits, J.B. Mudde, J. van de Belt, M. Verheul, J. Olivier, J. Homberg, V. Guryev, A.R. Cools, B.A. Ellenbroek, R.H. Plasterk, and E. Cuppen, Generation of gene knockouts and mutant models in the laboratory rat by ENU-driven target-selected mutagenesis, *Pharmacogenet Genomics* 16 (2006), 159-169

[51] B. Evers, and J. Jonkers, Mouse models of BRCA1 and BRCA2 deficiency: past lessons, current understanding and future prospects, *Oncogene* 25 (2006), 5885-5897

[52] M.S. Cotroneo, J.D. Haag, Y. Zan, C.C. Lopez, P. Thuwajit, G.V. Petukhova, R.D. Camerini-Otero, A. Gendron-Fitzpatrick, A.E. Griep, C.J. Murphy, R.R. Dubielzig, and M.N. Gould, Characterizing a rat Brca2 knockout model, *Oncogene* 26 (2007), 1626-1635

[53] D.H. Yan, Y. Wen, L.K. Su, W. Xia, S.C. Wang, S. Zhang, L. Gan, D.F. Lee, B. Spohn, J.A. Frey, G.N. Hortobagyi, and M.C. Hung, A delayed chemically induced tumorigenesis in Brca2 mutant mice, *Oncogene* 23 (2004), 1896-1901

[54] B.M. Smits, and E. Cuppen, Rats go genomic, *Genome Biol* 7 (2006), 306

[55] J.M. Amos-Landgraf, L.N. Kwong, C.M. Kendziorski, M. Reichelderfer, J. Torrealba, J. Weichert, J.D. Haag, K.S. Chen, J.L. Waller, M.N. Gould, and W.F. Dove, A target-selected Apc-mutant rat kindred enhances the modeling of familial human colon cancer, *Proc Natl Acad Sci U S A* 104 (2007), 4036-4041

[56] A.R. Moser, H.C. Pitot, and W.F. Dove, A dominant mutation that predisposes to multiple intestinal neoplasia in the mouse, *Science* 247 (1990), 322-324

[57] G.J. Rowse, S.R. Ritland, and S.J. Gendler, Genetic modulation of neu proto-oncogene-induced mammary tumorigenesis, *Cancer Res* 58 (1998), 2675-2679

[58] D.J. Samuelson, S.E. Hesselson, B.A. Aperavich, Y. Zan, J.D. Haag, A. Trentham-Dietz, J.M. Hampton, B. Mau, K.S. Chen, C. Baynes, K.T. Khaw, R. Luben, B. Perkins, M. Shah, P.D. Pharoah, A.M. Dunning, D.F. Easton, B.A. Ponder, and M.N. Gould, Rat Mcs5a is a compound quantitative trait locus with orthologous human loci that associate with breast cancer risk, *Proc Natl Acad Sci U S A* 104 (2007), 6299-6304

Tables

Table 1: Histological and morphological analysis of transplanted mammary tissue

		Histological analysis of transplanted mammary tissue	
Donor ---> Recipient	**n**	**Hyperlobularity**	**Carcinoma**
Brca2$^{+/+}$ --->*Brca2*$^{+/+}$	6	0	1[a]
Brca2$^{-/-}$ ---> *Brca2*$^{+/+}$	11	3	0

		Morphological analysis of transplanted mammary tissue				
Donor ---> Recipient	**n**	**Degree of branching**			**Degree of lobularity**	
		Low	**High**	**Both**	**Low**	**High**
Brca2$^{+/+}$ --->*Brca2*$^{+/+}$	8	7	0	1	8	0
Brca2$^{-/-}$ ---> *Brca2*$^{+/+}$	17	8	6	3	9	8

[a] Note, the only carcinoma that developed in this experiment was in a wild type animal.

Table 2: Summary of genetically engineered rat models for breast cancer

Gene	**Promoter**	**Technology**	**Pathological mammary phenotype**	**Ref.**
Hs *neu*	MMTV	transgenic	>70% of multiparous females develop hyperplastic lesions, and stochastically DCIS and carcinomas; no lesions in virgin animals	[18]
Rn *neu*	MMTV	transgenic	Carcinomas in 100% of intact TG males, 100% of androgen treated TG males, and ~80% of androgen treated TG females	[19]
Rn *Ha-ras*/*K-ra*s	Rn *Ha-ras*	transgenic	No pathological mammary abnormalities; resistance to NMU-induced mammary tumor multiplicity	[32]
Hs *Ha-ras*	Hs *Ha-ras*	transgenic	NMU- / DMBA- induced mammary carcinogenesis, independent of increased amount of activating mutations in the transgene	[33,34]
Rn *neu**	MMTV	infusion	DCIS-like hyperplasias and invasive mammary carcinomas develop that resemble human pathology and hormone-sensitivity/dependence	[35,36]
Rn *Ha-ras*/K-ras**	MMTV	infusion	Activated *Ha-ras* is 10-fold more potent in the induction of mammary carcinomas than *K-ras*	[41]
Rn *Brca1/Brca2*	-	knockout	No increased mammary carcinogenesis susceptibility; *Brca2* was tested in various tumor inducing experimental settings	[49,52]

* activated form

Hs = *Homo sapiens*; Rn = *Rattus norvegicus*; MMTV = Moloney mammary tumor virus; DCIS = Ductal Carcinoma In Situ; TG = transgenic; NMU = nitrosomethylurea; DMBA = *7,12*-dimethylbenz[a]anthracene

Figure Captions

Figure 1: Hematoxylin and eosin staining of paraffin sections showing progression of mammary lesions following infusion of the pJR-*neu* retroviral vector in Wistar Furth rats. (A) Mammary tissue from an adult rat, showing normal ductal epithelium. (B) Intraductal cribriform hyperplasia seen two weeks after infusion. (C) Mammary lesion (two weeks post-infusion) resembling comedo type ductal carcinoma in situ (DCIS) with arrow pointing to necrosis. (D) Carcinoma, 12 weeks post-infusion. All photos were taken at 20X magnification.

Figure 2: Aluminum carmine staining of transplanted mammary tissue from (A) *Brca2*$^{+/+}$ donor showing minimal branching and lobularity and from (B) *Brca2*$^{-/-}$ donors showing hyperlobular phenotype. Mammary glands from 4-week-old donors were pooled, minced and surgically transplanted into the subscapular fat pads of *Brca2*$^{+/+}$ recipients and removed after 1 year. Photographs taken at 4X magnification.

Figures

Figure 1:

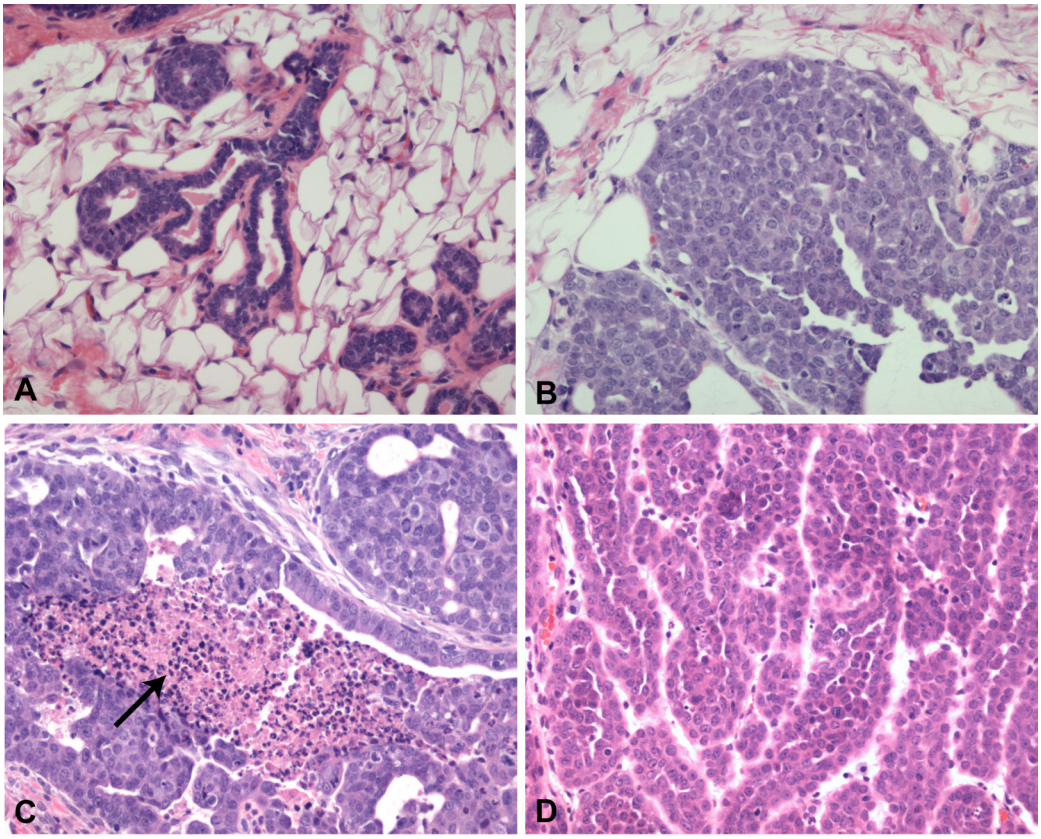

Figure 2: